

FAI/93-25

**D. C. COOK NUCLEAR PLANT
HYDROGEN CONTROL EVALUATION
SUMMARY REPORT**

Submitted to:

**American Electric Power Service Corporation
Columbus, Ohio**

Prepared by:

**Fauske & Associates, Inc.
16W070 West 83rd St.
Burr Ridge, IL 60521**

February 1993

9303030126 930226
PDR ADCK 05000315
P PDR

D. C. COOK NUCLEAR PLANT
HYDROGEN CONTROL EVALUATION
SUMMARY REPORT

TABLE OF CONTENTS

	<u>Page</u>
LIST OF TABLES	iii
LIST OF FIGURES	iv
ABSTRACT	vi
1. INTRODUCTION	1-1
1.1 Containment Design	1-1
1.2 Hydrogen Control System for Severe Accident	1-2
2.0 ACCIDENT SEQUENCE ANALYSIS METHODOLOGY	2-1
2.1 Accident Sequence Selection	2-1
2.2 MAAP Code and Accident Sequence Modeling	2-5
2.2.1 Hydrogen Generation	2-5
2.2.2 Recoverability Criterion	2-11
2.2.3 Combustion Models	2-12
2.2.4 Ignition Criteria	2-14
3.0 SEQUENCE ANALYSIS AND RESULTS	3-1
3.1 Low Pressure Scenario: Large Break LOCA	3-1
3.2 Intermediate Pressure Scenario: Small Break LOCA	3-2
3.3 High Pressure Scenario: Loss of Component Cooling Water Accident	3-12
4.0 SENSITIVITY ANALYSIS	4-1
4.1 Two Operating Fans	4-1
4.2 Fan Failure	4-3
4.3 Core Power and Fuel Configuration	4-6
4.4 Station Blackout	4-10
5.0 SUMMARY AND CONCLUSIONS	5-1
REFERENCES	

LIST OF TABLES

<u>Table</u>		<u>Page</u>
2.1-1	Dominant Cook Nuclear Plant Functional Sequences	2-1
2.1-2	Cook Nuclear Plant Candidate Functional Sequences and Initiators For 10CFR50.44 Analysis	2-3
2.1-3	Selected Accident Scenarios for 10CFR50.44 Analysis	2-4
2-1	Examples of Important Plant Data and Their Location in the Cook MAAP Parameter File	2-6
3-1	D. C. Cook Nuclear Plant 10CFR50.44 MAAP Analysis Base Case Summary	3-2
4-1	D. C. Cook Nuclear Plant 10CFR50.44 MAAP Analysis Sensitivity Case Summary	4-2
4-2	Base Case Peak H ₂ Concentrations	4-5
4-3	Core Configuration of Unit 1 and Unit 2	4-9

LIST OF FIGURES

<u>Figure</u>	<u>Page</u>
2-1	MAAP nodalization of the Cook Primary System 2-8
2-2	MAAP nodalization of Cook containment (volumes and intercompartmental flow areas are shown) 2-9
2-3	MAAP flammability limit fit at elevated temperatures 2-13
2-4	HECTR burn completeness model as a function of H ₂ concentration 2-15
3.1a	Primary system pressure and reflood rate during large LOCA 3-4
3.1b	Hydrogen generation rate and cumulative hydrogen generation during large LOCA 3-5
3.1c	Steam and hydrogen concentrations in the lower compartment during large LOCA 3-7
3.1d	Upper compartment pressure and lower compartment equipment temperature during large LOCA 3-8
3.2a	Primary system pressure and reflood rate during small LOCA 3-10
3.2b	Hydrogen generation rate and cumulative hydrogen generation during small LOCA 3-11
3.2c	Steam and hydrogen concentrations in the lower compartment during small LOCA 3-13
3.2d	Upper compartment pressure and lower compartment equipment temperature during small LOCA 3-14
3.3a	Primary system pressure and reflood rate during loss of CCW 3-17



LIST OF FIGURES

<u>Figure</u>	<u>Page</u>
3.3b	Hydrogen generation rate and cumulative hydrogen generation during loss of CCW 3-18
3.3c	Steam and hydrogen concentrations in the lower compartment during loss of component cooling water 3-20
3.3d	Upper compartment pressure and lower compartment equipment temperature during loss of CCW 3-21
4.2a	Hydrogen concentrations in upper compartment and upper plenum during base cases 4-4
4.2b	Hydrogen concentrations in upper compartment and upper plenum during loss of CCW with recirculation fan failure 4-7
4.2c	Upper compartment pressure and equipment temperature in the lower compartment during loss of component cooling water with fan failure 4-8
4.3a	Hydrogen generation rate and cumulative hydrogen generation during Unit 2 large LOCA 4-11
4.3b	Hydrogen concentrations in upper compartment and upper plenum during Unit 2 large LOCA 4-12
4.3c	Upper compartment pressure and equipment temperature in lower compartment during Unit 2 large LOCA 4-13
4.4a	Hydrogen generation rate and cumulative hydrogen generation during station blackout 4-16
4.4b	Upper compartment pressure and lower compartment equipment temperature during station blackout 4-17



ABSTRACT

This report provides the results of a hydrogen control evaluation and its technical bases for the D. C. Cook Nuclear Plant in support and demonstrating compliance with 10CFR50.44, Section (c) (3) (vi) (A).

The rule requires that the containment structural integrity be maintained and an equipment necessary for a safe shutdown be survived and maintained. The total amount and the rate of hydrogen generation, both of which depend on the rate of water supply during the recovery phase, are critical to the ability to satisfy these requirements.

In this study, a wide range of core reflood rates as determined by the possible range of the primary system pressure at the time of reflood are taken into account. Accident scenarios analyzed in this study are selected from dominant sequences identified by the Cook Nuclear Plant Individual Plant Examination efforts. The analysis is performed with the MAAP code.

Title 10 of the Code of Federal Regulations (10CFR), Section 50.44, "Standards for Combustible Gas Control System in Light-Water-Cooled Power Reactors," requires that a hydrogen control system be provided and the system be capable of accommodating, without loss of containment structural integrity, the amount of hydrogen generated from a metal-water reaction up to 75 percent of the active fuel cladding following an accident. In addition, systems and components necessary to establish and maintain safe shutdown must be capable of performing their function regardless of hydrogen burning.

Paragraph (c) (3) (vi) (A) of the hydrogen rule (10CFR50.44) specifies that pressurized light-water nuclear power reactors with an ice-condenser type of containment submit an analysis to the commission evaluating the consequences of large amounts of hydrogen following the start of an accident. Paragraph (c) (3) (vi) (A) (3) requires the analysis to utilize accident scenarios accepted by the NRC staff.

The D. C. Cook Nuclear Plant uses an ice-condenser type of containment and is subject to the hydrogen rule (10CFR50.44). The purpose of this report is to provide a portion of the analysis needed to demonstrate compliance with the hydrogen rule for the D. C. Cook Nuclear Plant including its hydrogen control system.

1.1 Containment Design

The Donald C. Cook Nuclear Plant containment building is a steel lined, reinforced concrete cylindrical structure with a hemispherical dome and a flat basemat. The containment building is partitioned into several compartments consisting of a total free volume of approximately 1,300,000 cubic feet. The lower compartment houses the reactor pressure vessel and the reactor coolant system. The intermediate compartment contains the energy absorbing ice bed which condenses steam that is generated in the lower compartment during a Loss of Coolant Accident (LOCA). The upper compartment consists of the very open volume above the refueling floor that accommodates the air that is displaced from the other two volumes during an accident scenario. The condensation of steam in the ice condenser limits the containment pressure to values substantially below those for other large, dry PWR containments. During an accident, these compartments communicate via a network of recirculation fans which are designed to force the heat released in the lower compartment up through the ice condenser, into the upper compartment, and then back into the lower compartment. The ultimate pressure capacity of the containment was analyzed extensively during its IPE efforts. A 95/95 confidence value is 36 psig [AEPSC, 1981].

1.2 Hydrogen Control System for Severe Accidents

The D. C. Cook Nuclear Plant employs a Distributed Ignition System (DIS) consisting of thermal igniters control hydrogen in the case of a severe accident. In addition, an Air Recirculation and Hydrogen Skimmer System is used to meet the hydrogen control requirements of a design basis accident.

The D. C. Cook Nuclear Plant DIS utilizes seventy (70) GMAC-7G glow plug igniters within containment, distributed throughout the various containment compartments. These glow plugs are very reliable at igniting hydrogen concentrations near the lower flammability limit. They require only twelve (12) to twenty (20) seconds before reaching the hydrogen ignition temperature ($\sim 1550^{\circ}\text{F}$). These igniters have been positioned to assure adequate spatial coverage in those areas of containment to which hydrogen could be released or where it could flow in significant quantities. The general criteria for placement of igniters are as follows:

- The igniters are above the maximum floodup level within containment.
- At least two igniters, controlled and powered redundantly, are located in each region of concern.
- Igniter locations are in areas which should be well mixed by the air recirculation/hydrogen skimmer system and/or by blowdown forces.
- Igniters are placed about one-third of the way up a wall within a compartment, in order to maximize the amount of hydrogen combusted via upward propagation in a lean mixture. Exceptions are made for the upper plenum of the ice condenser and areas with concentrations of instrumentation.
- Placement of igniters in the upper plenum of the ice condenser involves other considerations. For hydrogen concentrations on the order of 8% by volume, the downward propagation is possible due to the turbulence in the flow stream upon exit from the ice condenser. In order to take advantage of both the upward and downward propagation characteristics of flow streams, placement of the igniters two-thirds of the way up the wall in the upper plenum is appropriate.

Following a degraded core accident in which hydrogen is liberated to the lower compartment, there are twenty four (24) igniters strategically positioned throughout the lower compartment which are expected to provide the first defense against hydrogen accumulation. Two igniters are located in each steam generator and pressurizer enclosure. These igniters are positioned near the top of the enclosures to account for potential hydrogen pocketing concerns. Two igniters

are also positioned near the Pressurizer Relief Tank (PRT) in case the PRT rupture disk blows and provides a possible hydrogen escape route from the primary system.

It is expected that the lower compartment igniters will not result in the burning of all the hydrogen in that compartment, due to steam inertia or other mechanisms. Once this steam-hydrogen mixture passes through the ice bed, the mixture may become flammable once it reaches the ice condenser upper plenum. For this reason, a total of fourteen (14) igniters are located in the upper plenum. Additionally, twelve (12) igniters are located in the dome area of the upper compartment. These igniters are expected to aid in the control of any hydrogen which escapes the ice condenser upper plenum.

Additional control of hydrogen during air recirculation is afforded by ten igniters mounted on the exterior of the steam generator and pressurizer enclosures in the upper compartment. Four igniters are mounted in each of the two fan/accumulator rooms as potential hydrogen pocketing areas. Two igniters are also located in the instrument room.

The DIS is a manual system controllable from the main Control Room.

2.0 ACCIDENT SEQUENCE ANALYSIS METHODOLOGY

2.1 Accident Scenario Selection

To meet the objectives of 10CFR50.44 in selecting accident scenarios, the Cook Nuclear Plant IPE was utilized as a starting point for identifying sequences. The spectrum of sequences analyzed for the IPE would describe the behavior of the reactor system under a broad range of system configurations.

The following delineates the method utilized to select the 10CFR50.44 accident scenarios:

1. Tabulate the IPE functional sequences by frequency of occurrence.
2. Screen the tabulated functional sequences retaining only those with a frequency of occurrence greater than or equal to 10^{-6} . The screening criteria is based on the NUMARC guidelines [NUMARC, 1992].
3. Review the resultant list of functional sequences for applicability to the 10CFR50.44 analysis, justifying the deletion of any sequences.
4. For the remaining functional sequences, select the top systemic sequence initiator and evaluate for applicability to the 10CFR50.44 analysis.

Steps 1 and 2 above produced the following functional sequences:

Table 2.1-1

Dominant Cook Nuclear Plant Functional Sequences

<u>Functional Sequence</u>	<u>Frequency of Occurrence (per year)</u>
SLR	1.507×10^{-5}
THR	1.648×10^{-5}
SHR	2.098×10^{-5}
THWIF	1.0763×10^{-6}
ALR	1.596×10^{-6}
GHR	5.99×10^{-6}



The functional sequences are identified through a series of designators, the first of which addresses the initiator. These initiator designators are

- T - Transient
- S - Small primary system break
- A - Large primary system break
- G - Steam generator tube rupture

The second designator addresses RCS pressure at time of vessel failure. High Pressure (H) indicates the failure pressure is above the low head injection shut-off head. Low pressure (L) indicates RCS pressure is below low head injection.

The series of designators following the initiator and RCS pressure identify the status of ECCS injection and containment heat removal. These ECCS designators are

- W - No RWST injection into the vessel
- C - Successful containment spray injection and failed spray recirculation
- R - Successful containment spray injection and recirculation
- I - Failed hydrogen igniters
- F - Failed containment recirculation fans

Functional sequence THWIF constitutes failed igniters. One of the objectives of 10CFR50.44 is to demonstrate the adequacy of combustion control systems. Failing the igniters would not achieve this objective. Thus, the THWIF functional sequence is deleted. Functional sequence GHRC is a steam generator tube rupture. Systemic sequences in this group progress to a bypass of the containment. This type of scenario is not conducive to analyzing combustible gas control within containment and thus functional sequence GHR is also deleted from further consideration.

The remaining functional sequences are tabulated in Table 2.1-2 along with a listing of their top systemic sequence initiators. The top systemic initiators are all those initiators of systemic sequences above a cut-off frequency of 10^{-9} .

TABLE 2.1-2

Cook Nuclear Plant
Candidate Functional Sequences and Initiators
For 10CFR50.44 Analysis

<u>Functional Sequence</u>	<u>Initiators</u>
SLR	Small LOCA Medium LOCA
THR	Loss of component cooling water Loss of essential service water Loss of DC Steam line break Station blackout Transient with steam conversion Loss of offsite power Transient without steam conversion ATWS
SHR	Small LOCA ATWS Medium LOCA
ALR	Large LOCA Vessel failure

The challenge to the containment integrity due to hydrogen combustion would depend on hydrogen generation rate and the amount generated during the accident scenarios. As discussed later in Sections 2.2.1 and 2.2.2, the reflood rate during core recovery is the factor determining the in-vessel hydrogen generation rate from the cladding steam reaction. However, the ability to reflood depends on the RCS pressure. Hence, the selected accident scenarios should cover the possible range of the RCS pressure at reflood. The challenge to long term decay heat removal would depend on survivability of critical instrumentations during hydrogen burns. The mitigation from severe burns could be provided if instrumentations are submerged under water as a result of RWST injection into the containment. Inspection of Table 2.1-2 shows that all the candidate functional sequences have equal footing on water accumulation in the lower compartment since containment spray injection from the RWST is successful in all these sequences. Therefore, the criteria for selecting accident scenarios can be based on primary system pressure and likelihood of occurrence. The results are accident scenarios at low, intermediate, and high pressures as shown in Table 2.1-3. The low pressure scenario is bounded by the top initiator of functional sequence ALR (large LOCA). The intermediate pressure scenario is represented by the top initiator of functional sequence SHR (small LOCA). The high pressure scenario is represented by the top initiator of functional sequence THR (loss of component cooling water). All selected accident scenarios for 10CFR50.44 analysis are shown in Table 2.1-3.

Table 2.1-3

Selected Accident Scenarios for 10CFR50.44 Analysis

<u>Selected Accident Scenario with Recovery Actions</u>	<u>Primary System Pressure at Recovery</u>
1. Large LOCA	Low
2. Small LOCA	Intermediate
3. Loss of Component Cooling Water	High

2.2 MAAP Code and Accident Sequence Modeling

The Modular Accident Analysis Program (MAAP) provides an integrated approach to modeling reactor thermal hydraulics and containment response including in-vessel hydrogen generation, in-containment hydrogen transport and combustion phenomena during postulated accidents. The MAAP code used in this study is the code version (MAAP 3.0B, PWR Rev. 17.02) used in the Cook Nuclear Plant IPEs [Fauske & Associates, 1991], with selected modifications to the hydrogen generation and combustion models to support the study. This section describes modifications that were made specifically for the Cook Nuclear Plant 10CFR50.44 hydrogen analysis. Other detailed documentation of the standard MAAP code can be found in the MAAP 3.0B Users Manual [Fauske & Associates, 1990].

MAAP requires plant-specific input data in the form of a MAAP parameter file. A Cook Nuclear Plant-specific parameter file was developed as part of the Cook Nuclear Plant IPE effort, and is used in this study. This plant-specific parameter file and its supporting documentation are included in the Cook Nuclear Plant Containment Data Collection Notebook [Fauske & Associates, 1992]. Table 2-1 shows correlations of important plant data to the parameter file sections.

Nodalization of the primary system is illustrated in Figure 2-1. Among the 4 coolant-steam generator loops, 3 "unbroken" loops are lumped and treated together as one loop. The "broken" loop containing the primary system break is treated separately from the "unbroken" loop. Except the core, there are 13 nodes representing the primary system. Each node has an individual gas temperature, hydrogen mass fraction and up to 4 structure temperatures. The core is a multi-node volume consisting of 70 nodes. Treatment of gas transport within the primary system includes hot leg counter-current flow, unidirectional flow between nodes and gas flow at the primary system break(s).

The containment is nodalized into 6 regions representing the upper compartment, the lower compartment, the annular (deadend) compartment, the ice condenser, the upper plenum of the ice condenser, and the cavity. Containment nodalization is illustrated in Figure 2-2. In each region, pressures, temperatures, miscellaneous thermodynamic properties and fission products are calculated based on the production and transport of mass and energy in the region. Intercompartmental flows are calculated from a combination of fan flows, pressure-driven flows and natural convection flows.

2.2.1 Hydrogen Generation

The primary source of hydrogen generation during degraded core accidents in light water reactors (LWRs) is due to the oxidation of Zircaloy fuel-rod cladding by steam [Cronenberg, 1990]. The oxidation process is represented by the following exothermic chemical reaction:

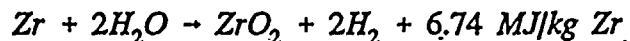


Table 2-1

Examples of Important Plant Data and Their Location
in the Cook MAAP Parameter File

<u>Plant Data</u>	<u>Parameter File Section</u>
Reactor Core (full power, UO2 mass, Zr mass, mass of lower core plate and core support plate, fuel enrichment, fuel geometry)	*Core
Reactor Vessel (vessel mass, volume, wall thickness, mass of core barrel, upper plenum internals, geometry)	*Primary System
Primary System (hot & cold legs, volumes, elevations, scram set pts)	*Primary System
Primary System (initial water level, P,T)	*Initial Conditions
Pressurizer Details	*Pressurizer
Quench Tank Details	*Quench Tank
Steam Generator Details	*Steam Generator
Accumulators (water mass, temperature)	*Engineered Safeguards
Ice Condenser	*Ice Condenser
Ice Condenser Upper Plenum	*Upper Plenum (UCOMPT)
Containment Structure (volumes, areas and thicknesses, elevations, equipment mass, heat sinks, liner thickness, failure pressure)	*Upper Compartment (ACOMPT) *Lower Compartment (BCOMPT) *Annular Compartment (DCOMPT)
Containment Structure (cavity volume, floor area, basemat thickness)	*Cavity (CCOMPT)
Containment Structure (concrete properties, composition, rebar density)	*Concrete and Containment Shell

Table 2-1 (Continued)

Examples of Important Plant Data and Their Location
in the Cook MAAP Parameter File

<u>Plant Data</u>	<u>Parameter File Section</u>
Containment Normal Conditions (T, P)	*Initial Conditions
Containment Systems (recirculation fans, sprays, spray HX)	*Engineered Safeguards
ECCS Injection/Recirculation (RWST water mass & temperature, charging, high-pressure and low-pressure injection, RHR HX details, pump curves, set points)	*Engineered Safeguards



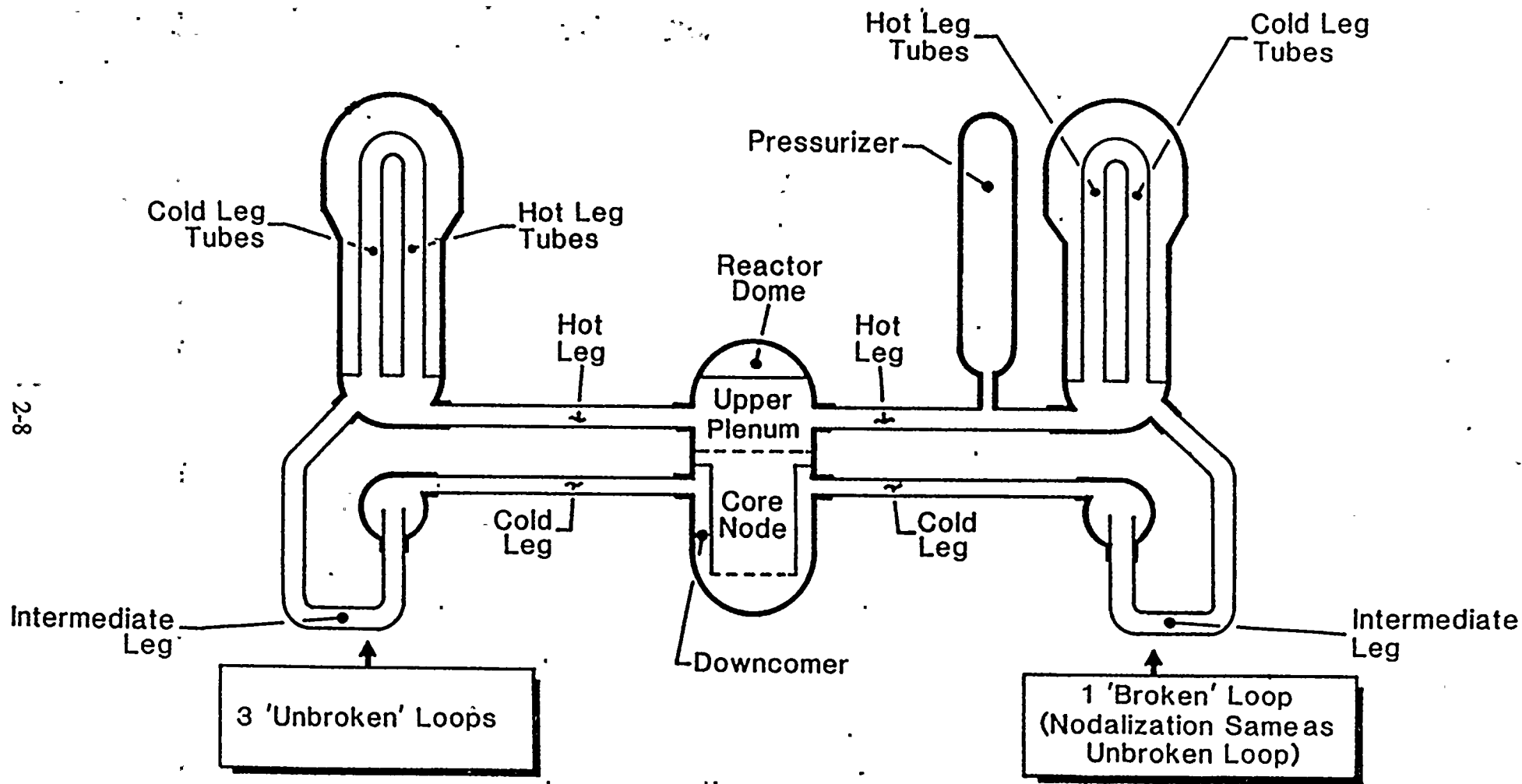
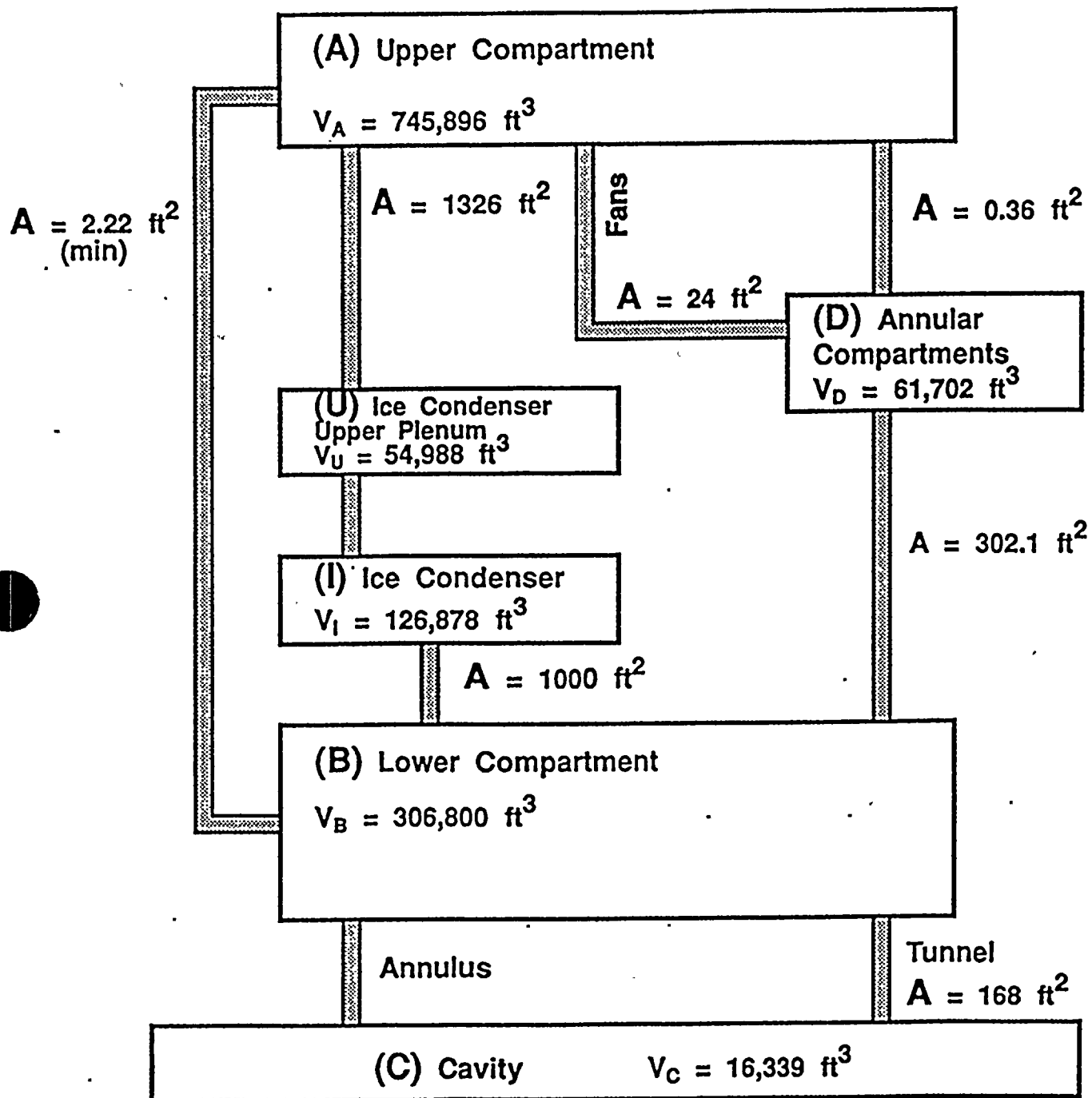


Figure 2-1 MAAP nodalization of the Cook Primary System.



JB923071.CDR

Figure 2-2 MAAP nodalization of Cook containment (volumes and intercompartmental flow areas are shown).

The Cook Nuclear Plant Unit 1 reactor contains 43521.5 lbs of zirconium in the fuel-rod cladding [Fauske & Associates, 1992]. An oxidation reaction of 75% of the cladding, as required by the hydrogen rule 10CFR50.44, would produce approximately 1430 lbs of hydrogen. Cook Nuclear Plant Unit 2 has a different fuel design with less total zirconium but more surface area (17 x 17 fuel rod array vs. 15 x 15). Unit 2 is the subject of a sensitivity analysis in Section 4.

Hydrogen production through clad oxidation can occur in an overheated core with boildown occurring first and recovery through reflooding of the vessel. The hydrogen generation rate during the two stages differ in their characteristics.

For the boildown stage, following depletion of water within the core during an accident sequence, overheating of the fuel pin cladding in the presence of steam would result in oxidation of the Zircaloy cladding. If the water level decreases further such that only the lower regions of the core would be covered, the steam supply rate would be reduced and the oxidation rate would be limited by the steam generation rate. If the decrease in the water level continues and the core heats up further, the energy release rate increases. Eventually, the cladding would reach a molten state due to both decay heat and heat of oxidation. Melting and relocating of molten core materials, and deformation of the original core configuration would reduce the surface area available for oxidation and may eventually block the steam and hydrogen flow to the overheated portion.

For the recovery stage, a higher hydrogen generation rate would be expected. Once water is injected to submerge and quench the overheated core, steam will again be created. The steam produces two competing effects. First, the steam enhances the Zircaloy oxidation processes which becomes a heat source to sustain or increase core temperatures which in turn increases the oxidation rate. Secondly, the steam provides a heat removal mechanism for the overheated and uncovered fuel rods. These competitive processes control the hydrogen generation rate and the total amount of hydrogen produced during reflood as a function of the reflood rate. A high reflood rate which quickly quenches and refills the core tends to produce a high peak generation rate but less total hydrogen. Experiences from the TMI-2 accident suggest that the extent of oxidation is likely greatest during the reflood conditions but is substantially lower than 50% prior to the onset of a recovery state [Henrie, 1989].

The Hydrogen Control Owners Group (HCOG), which performed extensive studies related to the reflood of an overheated and partially oxidized core in support of the licensing basis for the MARK III containments, also concluded that the estimated amount of cladding-steam reaction for a recoverable core with a reflood rate ranging from 150 gpm to 5,000 gpm is far less than the 75% value required by the hydrogen rule 10CFR50.44 [U.S. NRC, 1990]. In the Safety Evaluation Report (NUREG-1417) related to the HCOG assessment, the NRC concludes that (1) mechanistic models cannot predict the required 75-percent cladding oxidation in the active fuel region without core damage beyond the recoverability criterion and (2) the use of a non-mechanistic release model based on heat balance is reasonable and acceptable. The non-mechanistic release rate used by the HCOG was 0.10 lbm of hydrogen per second [U.S. NRC, 1990].



In the HCOG analysis of hydrogen release rates, the boiling water reactor heatup code (BWR-CHUC) was used. The NRC's review of the BWR-CHUC code concludes that the overall modeling of the hydrogen generation rate in BWR-CHUC is reasonable and the total and peak hydrogen generation estimates are expected to be conservative [U.S. NRC, 1990].

In the MAAP 3.0B code, the HEATUP routine is responsible for calculation of in-vessel hydrogen generation. The Zircaloy oxidation model used in the HEATUP routine is based on work done by IDCOR [IDCOR, 1983]. In this model, two oxidation rate equations are used to calculate the rate of change of the oxide layer. The Cathcart rate equation [Cathcart, 1977] is used for Zircaloy temperature up to 1850 K and the Baker-Just rate equation [Baker and Just, 1962] is used for Zircaloy temperature above 1875 K. MAAP calculates the oxidation rate for temperatures between 1850 K and 1875 K by interpolation between the two rate equations. The HEATUP routine essentially predicts the same hydrogen generation profiles as the PWR CHC code developed by EPRI. The comparison study of the two codes is documented in the HEATUP/PWR section of the MAAP 3.0B Users Manual [Fauske & Associates, 1990].

MAAP's core nodalization permits up to 70 nodes. In this analysis, the core is modeled with 10 axial nodes and 7 radial nodes, and axial and radial power profiles are modeled accordingly. For each core node, mass and energy rate of change of UO_2 , Zr, ZrO_2 , H_2O and H_2 are calculated to determine the nodal mass and temperature. The water pool in the core is treated as a lumped control volume. The overall pool rates of change are determined by all inlet and outlet flows and by pool energy source terms. Steam and hydrogen are assumed to flow along the uncovered (and unblocked) flow channels. Mass flowrates and enthalpies in each channel are calculated by tracking the generation and consumption of Zr, ZrO_2 , H_2O and H_2 at each axial level. The channel exit values are summed to form a total steam and hydrogen flow from the core.

Similar to the HCOG analysis, MAAP 3.0B predicts in-vessel cladding oxidation for a recoverable core far below the 75% required by the hydrogen rule. To satisfy the 75% requirement, the MAAP analysis follows the HCOG approach using a non-mechanic release of 0.1 lbm/s to extend the hydrogen production to a value equal to the reaction of 75% of the active fuel pin cladding. The non-mechanistic "tail" in-vessel hydrogen generation is initiated as soon as the core is fully covered with water following reflood.

The MAAP 3.0B has been modified for the purpose of this analysis; to be able to supply a non-mechanistic "tail" in-vessel hydrogen generation at a rate specified by users [Fauske & Associates, 1993].

2.2.2 Recoverability Criterion

The analysis required by 10CFR50.44 is to be based on an accident that is limited to "recoverable" events. The criteria for determination of "recoverability" is not provided by the 10CFR50.44 rule. As such, a conservative definition of recoverability would be reasonable and acceptable. One such definition proposed by the HCOG and accepted by the NRC [U.S. NRC,



1990] is in terms of the fraction of Zircaloy that has reached or exceeded the Zircaloy melting temperature of 2170 K. The accepted melt fraction is 50%. The 50% Zircaloy melt fraction criterion in the NRC judgement is conservative. It assumes that retention of the original core geometry is unlikely after damage to the extent of 50% Zircaloy oxidation.

For the purpose of this analysis, the above criterion is used as a core recovery criterion. To achieve this in MAAP, the eutectic melting temperature of fuel is set to the Zircaloy melting temperature and the latent heat of fusion of fuel is set to a very large value such that core heatup never results in relocation of core materials. Thus, during reflood the core is in its original configuration and the overheated portion of the core does not exceed the Zircaloy melting temperature. The timing of reflood is chosen such that 50% of the core reaches the Zircaloy melting temperature.

2.2.3 Combustion Models

The MAAP 3.0B code is capable of simulating combustion phenomena and hydrogen transport within the containment during an accident sequence. The flammability limits of containment gas mixtures, burn duration, and burn completeness are all accounted for in the MAAP calculation of combustion of gases. Treatment of combustion in MAAP is assumed to be of deflagration type. Diffusion flames which could be established at the primary system break are not modeled.

The basis for the flammability limits in MAAP, is the construction of H_2 -Air-steam flammability limit curves that resemble those of [Hertzbert, 1981] and [Marshall, 1986]. The flammability limits are calculated as functions of volume fractions of air, hydrogen, and steam (as well as carbon monoxide and carbon dioxide if present), and temperature of the gas mixture (Figure 2-3). The calculation of the flammability limits by this method accounts for the effects of steam inerting. However, it does not account for the effects of fog inerting. Phenomenological uncertainties in predicting the effects of fog on the flammability limits will be accounted in the analysis through offset of the MAAP predicted flammability limits as described in the following section (Section 2.2.4).

The burn duration and burn completeness are calculated in MAAP based on the time and volume swept by an idealized propagating spherical fireball. The fireball is assumed to originate and grow upward (i.e., flame propagation) within an idealized vertically standing cylindrical volume whose radius and height are specified by users [Fauske & Associates, 1990]. The effective radius is determined from considerations of the actual configuration and dimensions of the containment compartment, while the effective height is normally determined from the distance between igniters and the compartment ceiling. The fireball growth is modeled as driven by the intrinsic laminar flame speed and buoyancy forces. The fireball propagation is terminated once it reaches the effective height. The time and volume swept by the fireball are used to calculate the burning rate. This burning rate is used to calculate the pressure rise. Calculation of flame burning velocity in MAAP is based on a product of a flame speed multiplier (to account for turbulence effects) and a sum of laminar flame speed and buoyancy-driven velocity. The

H2-AIR-H2O FLAMMABILITY

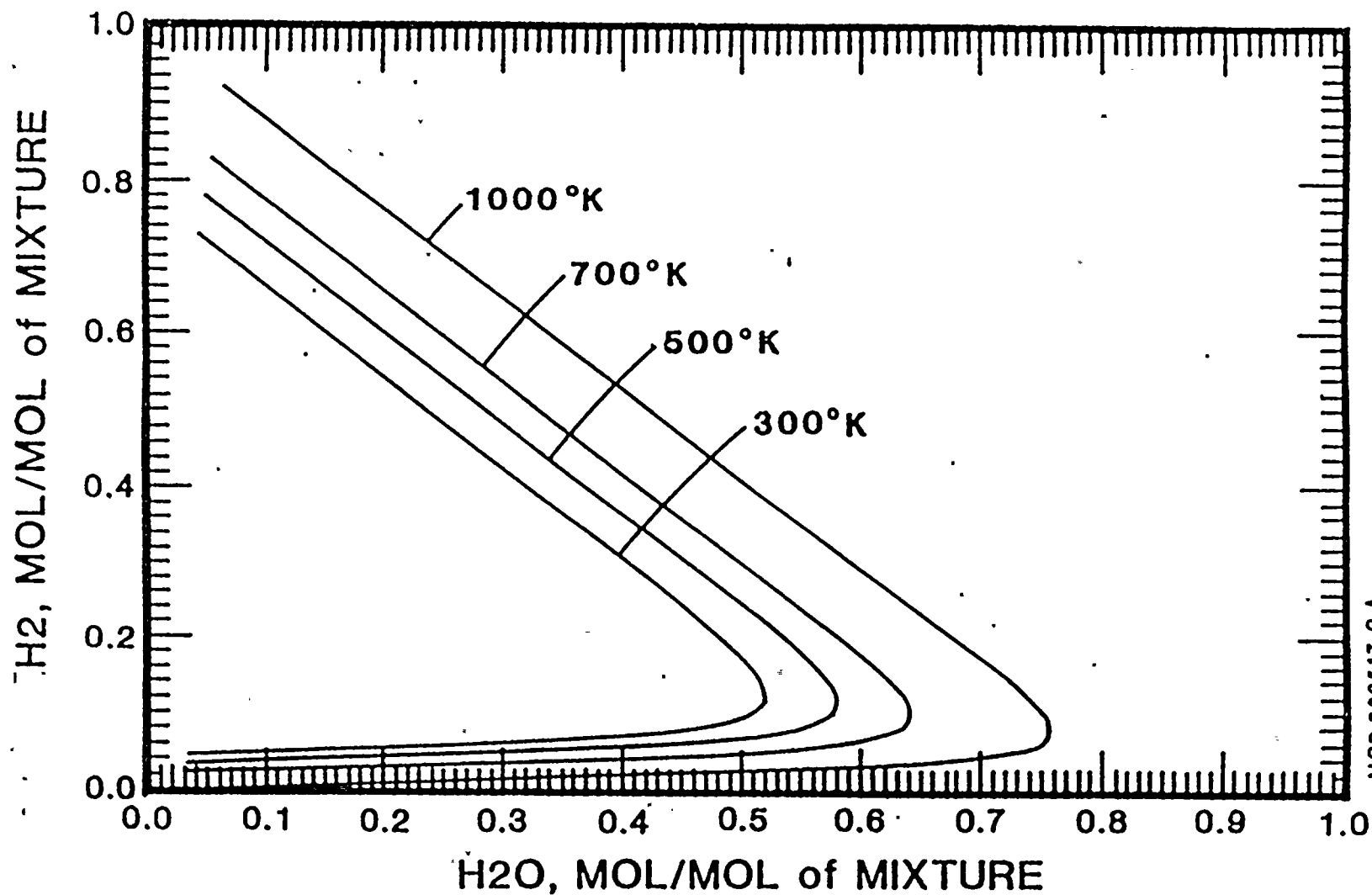


Figure 2-3 MAAP flammability limit fit at elevated temperatures.



laminar flame speed is calculated from a correlation proposed by [Liu, et al., 1981]. The correlation accounts for the effects of temperature and steam. The effects of pressure on laminar flame speed is calculated from the correlation of [Iijima & Takeno, 1986]. Good agreement with the NTS experiments with fans or sprays on has been shown by using a flame speed multiplier of 10 [Plys & Astleford, 1988]. A flame speed multiplier of 10 is assumed in this analysis.

Although the fireball approach treats flame propagation mechanistically, its accuracy depends on user-input effective radius and height. The determination of these parameters could become highly uncertain when dealing with the actual complicated configuration of the containment compartments and their distributed ignition system. To minimize uncertainties associated with the above approach, the MAAP code is specifically modified for the purpose of this study to incorporate the burn completeness correlation developed by Sandia National Laboratories and used in HECTR code version 1.5. The modification is documented in [Fauske & Associates, 1993]. Hence, in this analysis the burning rate is calculated based on the burn completeness predicted by the HECTR correlation and the burn duration predicted by the MAAP fireball propagation approach described above.

The HECTR correlation reads [EPRI, 1988]:

$$X_f = \text{MAX} [(1.8777 - 23.4397 X_i)X_i, 0.005X_i]$$

where X_f is final hydrogen mole fraction, X_i is initial hydrogen mole fraction, and the burn completeness is $(X_i - X_f)/X_i$. This correlation is shown in Figure 2-4 in comparison to available data including the NTS tests. The correlation predicts the upper limit of the burn completeness data. Hence, the use of this correlation results in a conservative estimate of combustion pressure and temperature rises.

2.2.4 Ignition Criteria

MAAP modeling of the distributed ignition system is treated through the determination of the normal flammability limits of the gaseous mixture of each containment region. The normal flammability limits are defined as the minimum hydrogen concentration required for the well mixed mixture of hydrogen, air and steam at a given steam concentration and temperature to be ignitable. When the normal flammability limit is satisfied, MAAP assumes the igniters would successfully ignite the mixture resulting in a deflagration through the compartment volume. However, due to a single node representation of each containment region, the ideally well mixed mixture of hydrogen, steam and air may not be established as assumed in the calculation. This non-ideal situation is more likely during a rapid release of hydrogen to the containment following reflood initiation. Furthermore, the effects of fog on the normal flammability limits must also be considered. Therefore, it is necessary to introduce ignition criteria which are defined as the minimum hydrogen concentration required for the non-ideal mixture in which fog may be present to be ignitable. Since MAAP calculates only the normal flammability limits, the ignition criteria



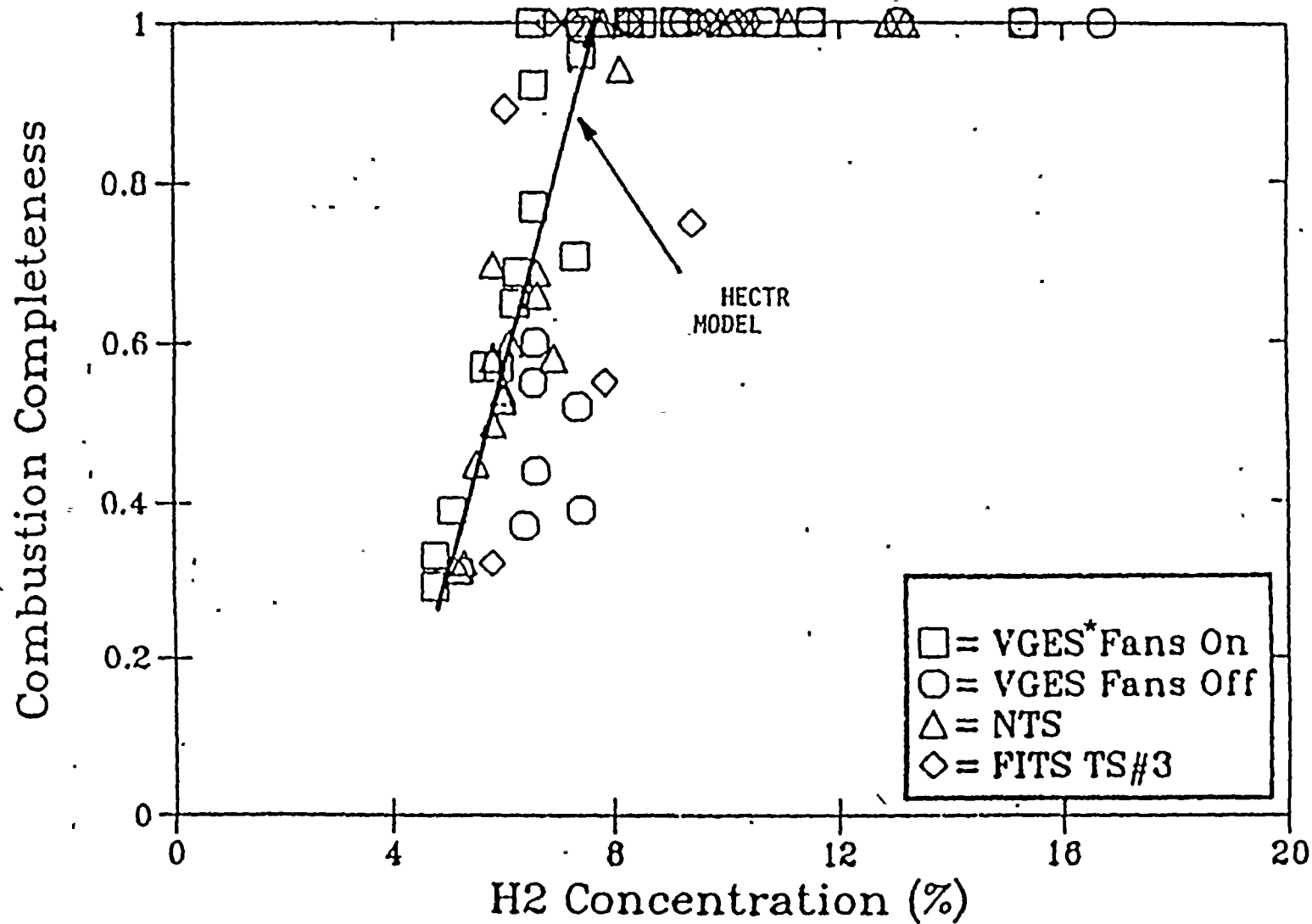


Figure 2-4 HECTR burn completeness model as a function of initial H₂ concentration.

*Variable-Geometry
Experimental System
(Sandia)

would be equal or higher than the MAAP predicted normal flammability limits. This section describes the modeling approach taken in this study.

Fog Inerting

Fog inerting is a unique issue relating to hydrogen combustion due to degraded core accidents in PWR ice condenser containments [Tsai & Liparulo, 1982]. The region expected to have the most fog inerting effecting its ignition system is the upper plenum of the ice condenser compartment. This is the result of its small volume and its downstream location to the ice condenser where fog is formed. Fog that may be present in other regions of the containment would be minimized by containment sprays. Steam condensation within the ice condenser generates small water droplets (i.e., fog) in the micron size range within the bulk of the gas stream. These small water droplets are carried by the gas stream into the upper plenum of the ice condenser where igniters are present to control hydrogen concentrations.

If high fog concentrations exist in the upper plenum, the minimum hydrogen concentration required for ignition would be higher than the normal flammability limits to compensate for heat loss to droplet vaporization. This would result in suppression of hydrogen burning in the upper plenum, and transport to and accumulation of hydrogen in the upper compartment. Depending on the level of fog inerting in the upper plenum, and on the hydrogen release rates during the accidents, ignition in the upper plenum may or may not occur at all. The consequence of hydrogen passing through the upper plenum without burning would likely lead to burning in other regions of the containment where fog inerting is less severe. Due to the large volume of the upper compartment (~ 55% of containment volume for Cook Nuclear Plant), any burn in the upper compartment, which initiates above the (lean) normal flammability limits, could create a sufficiently large pressure differential across the recirculation fan housing resulting in fan failure. On the other hand, the volume of the upper plenum is typically only 4 ~ 5% of the containment. Burns in the upper plenum normally result in negligible effects on the overall containment pressures and temperatures. Therefore, it is important that the effects of fog on the normal flammability limits are assessed in the analysis. The approach to fog assessment is described below.

Upper Plenum Region

The issue of fog inerting effects on hydrogen combustion in an ice condenser containment was extensively studied by Westinghouse [Tsai, 1981] and was recently revisited by [Luangdilok & Bennett, 1993] to theoretically quantify the fog inerting criteria in conjunction with ice condenser experiments. The conclusions in [Luangdilok & Bennett, 1993] suggest that for the worst scenario in which a maximum fog concentration is present in the upper plenum, the normal flammability limits in the upper plenum would be raised to between 7 vol.% and 8 vol.% H_2 . This value is quite consistent with the previous Cook Nuclear Plant hydrogen control study [AEPSC, 1985]. Depending on accident scenarios, the level of fog concentration would not exceed the worst scenario and the minimum H_2 concentration required to overcome fog inerting

References

1. Safety Evaluation Report transmitted by letter dated December 17, 1981, S.A. Varga [NRC] to J. Dolan [I&MCo].
2. "Donald C. Cook Nuclear Plant Units 1 and 2, Individual Plant Examination Summary Report," attachment to letter AEP:NRC:1082E, May 1, 1992.
3. Fauske & Associates, "Modular Accident Analysis Program", 1990; also "MAAP 3.0B Complete Code Manual," EPRI NP-777-1 CCML.
4. Letter AEP:NRC:500T dated October 8, 1985, M. P. Alexich [I&MECo] to H. R. Denton [NRC].
- 5 A. L. Camp, M. J. Wester, and S. E. Dingman, HECTR Version 1.0 User's Manual, NUREG/CR-3913, 1985.
- 6 S.E. Dingman, et al, HECTR Version 1.5 User's Manual, NUREG/CR-4507, April 1986.
7. L. B. Thompson, et al, Large-Scale Hydrogen Combustion Experiments, EPRI Report NP-3878, October 1988.
8. Safety Evaluation Report related to Hydrogen Control Owners Group Assessment of Mark III Containments, October 1990, NUREG-1417.
9. E. J. Eschbach, B. A. Ross, and W. K. Winegardner, Engineering Scale Ice Condenser Thermal Hydraulic Test Program, Battelle Pacific Northwest Laboratories, 1990.
10. W. Luangdilok and R. B. Bennett, "Fog Inerting Effects on Hydrogen Combustion in a PWR Ice Condenser Containment," to be published.
11. Letter AEP:NRC:0500A dated April 7, 1981, R. S. Hunter[I&MECo] to H. R. Denton [NRC], Attachment 1 contains a containment ultimate structural capacity report by Structural Mechanics Associates. A Safety Evaluation Report was written on this report and transmitted in a letter from S. A. Varga [NRC] to J. Dolan [I&MECo] on February 21, 1985.
12. Letter AEP:NRC:0500G dated February 17, 1982, R. S. Hunter [I&MECo] to H. R. Denton [NRC] (Attachment 2). This letter references Attachment 4 to letter dated December 1, 1981, L. M. Mills [TVA] to H. R. Denton [NRC], attention E. Adensam [NRC],

which provides information on equipment thermal response to temperature transients predicted by the CLASIX computer code.

13. J. A. Achenbach, R. B. Miller, and V. Srinivas, "Large Scale Hydrogen Burn Equipment Experiments", EPRI Report NP-4354, December 1985.

14. Letter AEP:NRC:500E dated July 2, 1981, R.S. Hunter [I&MECo] to H. R. Denton [NRC].

15. J. E. Shepherd, Analysis of Diffusion Flame Tests, NUREG/CR-4534, 1987.

16. K. D. Marx, Conchas-Spray Modeling of Flame Acceleration and Air Flows, Proceedings of the Thirteenth Water Reactor Safety Research Information Meeting, 1986.

would be bounded by 8 vol. % H_2 . Since suppression of hydrogen burning in the upper plenum may lead to fan failure and/or intensive burning in the lower containment region, it is conservative measure to assume ignition criterion at 8 vol. % H_2 in the upper plenum. This 8 vol. % H_2 ignition criterion for the upper plenum is employed in this study.

Regions Other Than Upper Plenum

Fog inerting in other regions is expected to be at a negligibly low level. To account for the non-ideal mixing of gases due to a single node representation of the containment region as discussed above, it will be assumed in this study that the gas mixtures in the regions other than the upper plenum are ignitable at 6 vol. % H_2 for the first burn in each region. The assumed ignition criterion of 6 vol. % H_2 is not unrealistically high and is conservative with respect to heat and pressure loads in the burning compartment since burning at 6 vol. % H_2 results in higher burn completeness than the normal flammability limits.

It is also assumed that following the first local (compartmental) burn in regions other than the upper plenum, the local (compartmental) ignition criterion is reduced to the normal flammability limits predicted by MAAP. This assumption accounts for the possibility of better mixing of gas mixture at later time, and the possibility of continuous burning in the regions as a result of continuous release of hydrogen to the containment. Continuous burning was observed in the NTS continuous injection tests [EPRI, 1988].

MAAP Modifications and Modeling of Ignition Criteria

The degree of fog inerting and non-ideal mixing of a combustible H_2 -air-steam mixture could vary significantly from one compartment to another. To account for such localized effects, the ability to locally offset the lean flammability limits for three regions was specifically added to the MAAP code for this study [Fauske & Associates, 1993]. The three regions are (1) upper plenum, (2) upper containment, and (3) lower containment (lower and annular compartments).

To model an 8 vol. % H_2 ignition criterion in the upper plenum, a 3.3% offset of the upper plenum lean flammability limits is assumed. This means that the lean flammability limits must equal or exceed 3.3% above the normal limits to be ignitable. This condition yields approximately an 8 vol. % H_2 ignition criterion. It is not a constant value since the flammability limits also depend on steam concentration and temperature. Similarly, a 1.1% offset of the lean flammability limits for other regions yield a 6 vol. % H_2 ignition criterion.

3.0 SEQUENCE ANALYSIS AND RESULTS

This section presents base case results from applying the MAAP code and assumptions as described in Section 2.2 to the accident scenarios selected in Section 2.1. The selected accident scenarios which are listed in Table 2.1-3 include a large break LOCA, a small break LOCA, and a loss of component cooling water. The scenarios represent a comprehensive spectrum of hydrogen generating events for Cook Nuclear Plant. The base case analyses are representative of Cook Nuclear Plant Unit 1 which has a higher Zircaloy inventory. Unit 2 is addressed in Section 4.0 "Sensitivity Analysis".

In all base case analyses, it is assumed that one train of containment sprays and one recirculation fan are available. It is also assumed that any burning occurs in the upper compartment will not result in fan failure. The impact of fan failure is addressed in the sensitivity analysis section. Major results of all base cases are summarized in Table 3-1. The peak equipment temperature represents the result of the calculation of a simple heat structure in the lower containment of 1/4" steel. This equipment temperature is used to identify sequences which may require a more detailed thermal analysis of limiting equipment or instrumentation. This additional analysis is beyond the scope of this report.

3.1 Low Pressure Scenario: Large Break LOCA Accident

A large LOCA accident represents a low pressure (~ 20 psia) scenario where the primary system pressure at the time of core recovery is sufficiently low to allow core recovery with high flowrate from the RHR pumps. In this scenario, the high recovery flowrate is 4500 gpm supplied by one RHR pump.

Core Recovery Criteria

The accident is initiated by a 4.0 sq. ft. (27 inch equivalent diameter) large break LOCA at the cold leg. Recovery of the heated core is delayed resulting in a 50% clad melt fraction. The following ECCS equipment is assumed operational during the accident scenario and are modeled accordingly in MAAP:

1. 3 of 3 accumulators inject to the cold legs
2. 1 of 2 RHR pumps inject to 1 of 3 intact cold legs
3. 1 of 2 trains of containment spray injection
4. Successful switch to containment spray recirculation
5. Low pressure recirculation using 1 RHR pump

Table 3-1
D. C. Cook Nuclear Plant 10CFR50.44 MAAP Analysis
Base Case Summary

Hydrogen Generation and Containment Parameters	Sequences		
	LLO	SLO	CCW
<u>Primary System</u>			
•Core Uncovery Time (hr)	0.62	1.84	2.75
•Vessel Reflood Time (hr)	0.93	2.4	3.53
•Pressure @ Reflood (psia)	17	1000	2300
<u>H₂ Generation rate (lb/s)</u>			
•Prior to Reflood	0.13	0.012	0.018
•During Reflood (average/peak)	2.93/8.1	0.58/5.0	0.45/3.0
•Artificial "tail"	0.1	0.1-	0.1
Reflood Transient Duration (min)	1.25	19	40
Reflood Rate (gpm)	4500	500	400 ~ 720
<u>Zr Oxidation (%)</u>			
•Prior to Reflood	7.8	1.1	2.2
•During Reflood	11.5	34.5	48.8
•Artificial "tail"	55.7	39.4	24.0
•Total	75.0	75.0	75.0
<u>Mass of H₂ Burned (lb)</u>			
•Upper Compartment	---	---	583
•Lower Compartment	160	340	231
•Annular Compartment	900	605	46
•I/C Upper Plenum	---	---	198
<u>Containment Peak Pressure (psia)</u>			
•Upper Compartment	21	19.3	28
<u>Peak Equipment Temperature (°F)</u>			
•Lower Compartment	234	192	217



6. 1 of 2 trains of hydrogen igniters in upper and lower containment regions
7. 1 of 2 containment recirculation fans.

Accident Scenario Description

The accident begins with a rapid blowdown of the primary system inventory into the containment which causes a rapid increase in containment pressure and a high gas temperature in the lower compartment region where the blowdown takes place. The maximum containment pressure during blowdown is 21 psi. The high containment pressure (above 2.9 psig) immediately actuates containment sprays and a recirculation fan (with a ten minute delay) to reduce the containment pressure. Within a half a minute after the break initiation, the blowdown is nearly complete and the primary system pressure drops below 400 psia. The resulting rapid depressurization of the primary system immediately activates accumulator injection and RHR injection into the vessel.

At 0.4 hours low level in the RWST is reached and the sprays are switched to the recirculation mode, RHR injection is assumed to fail on switchover to recirculation. Following ECCS failure, water in the reactor vessel rapidly drains out and boils away through the cold leg break, and the core uncovers at 0.62 hours. As the water level in the core decreases, the uncovered part of the core heats up and in-vessel hydrogen production due to Zircaloy cladding - steam reactions begins at 0.68 hours. About 148 lbm of hydrogen is produced prior to reflood. The peak generation rate before reflood is 1.3 lb/s while the average rate is about 0.13 lb/s. At 0.93 hours ECCS recirculation is assumed to be recovered, and the operators begin to reflood the reactor vessel with water. By this time about 89% of the core is uncovered. The portion of the uncovered core is assumed not to heat up beyond the melting point of Zircaloy (3447°F) by employing an artificially high latent heat of fusion of fuel in the analysis. Hence, during core reflood, cladding-steam reactions are assumed to occur at the maximum temperature limited by the Zircaloy melting point and the original core configuration is assumed intact rendering maximum surface and steam flow areas for reactions.

The kinetics of a Zircaloy cladding-steam reaction is so rapid that the factor limiting the reaction rate is the rate at which steam is supplied to the reaction surfaces. This rate depends on the core steaming rate which is proportional to the reflood rate. The reflood rate of this scenario is about the full flow capacity of one RHR pump (4500 gpm). This high flowrate can be realized because of the very low primary system pressure that exerts negligible resistance to the reflood flow (Figure 3.1a). The peak hydrogen generation rate during reflood is 8.1 lbm/s, while the average rate is about 2.93 lbm/s (Figure 3.1b).

Seventy-five seconds after reflood initiation, the core is fully recovered with water, terminating further in-vessel clad oxidation. The total in-vessel hydrogen generation until this time is 368 lbm, constituting 19.3% clad-water reactions. To satisfy the 75% clad-water reaction requirement, a non-mechanistic in-vessel hydrogen generation rate of 0.1 lbm/s is assumed as



D.C. COOK LARGE LOCA
BASE CASE ANALYSIS

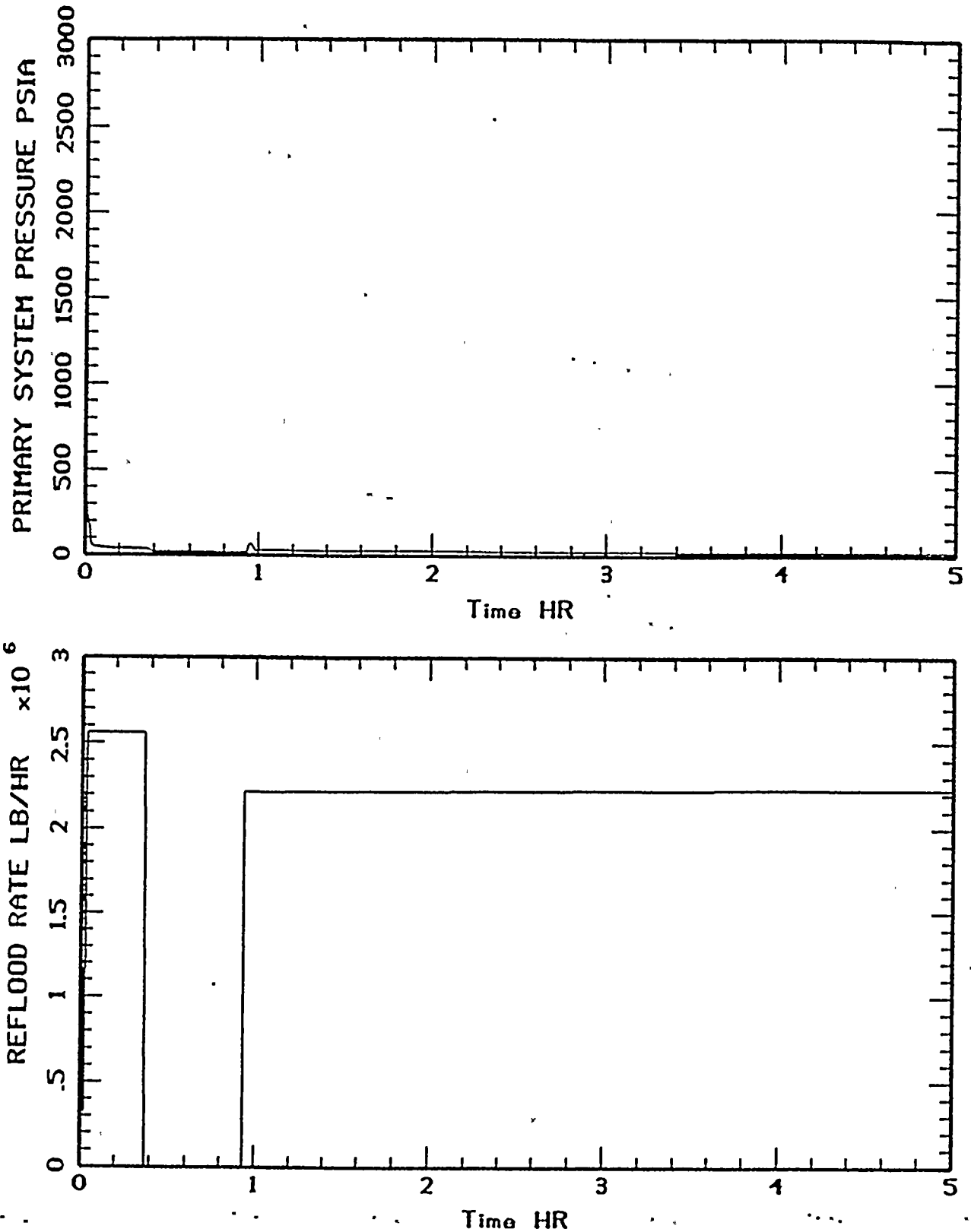


Figure 3.1a Primary system pressure and reflood rate during large LOCA.

D.C. COOK LARGE LOCA
BASE CASE ANALYSIS

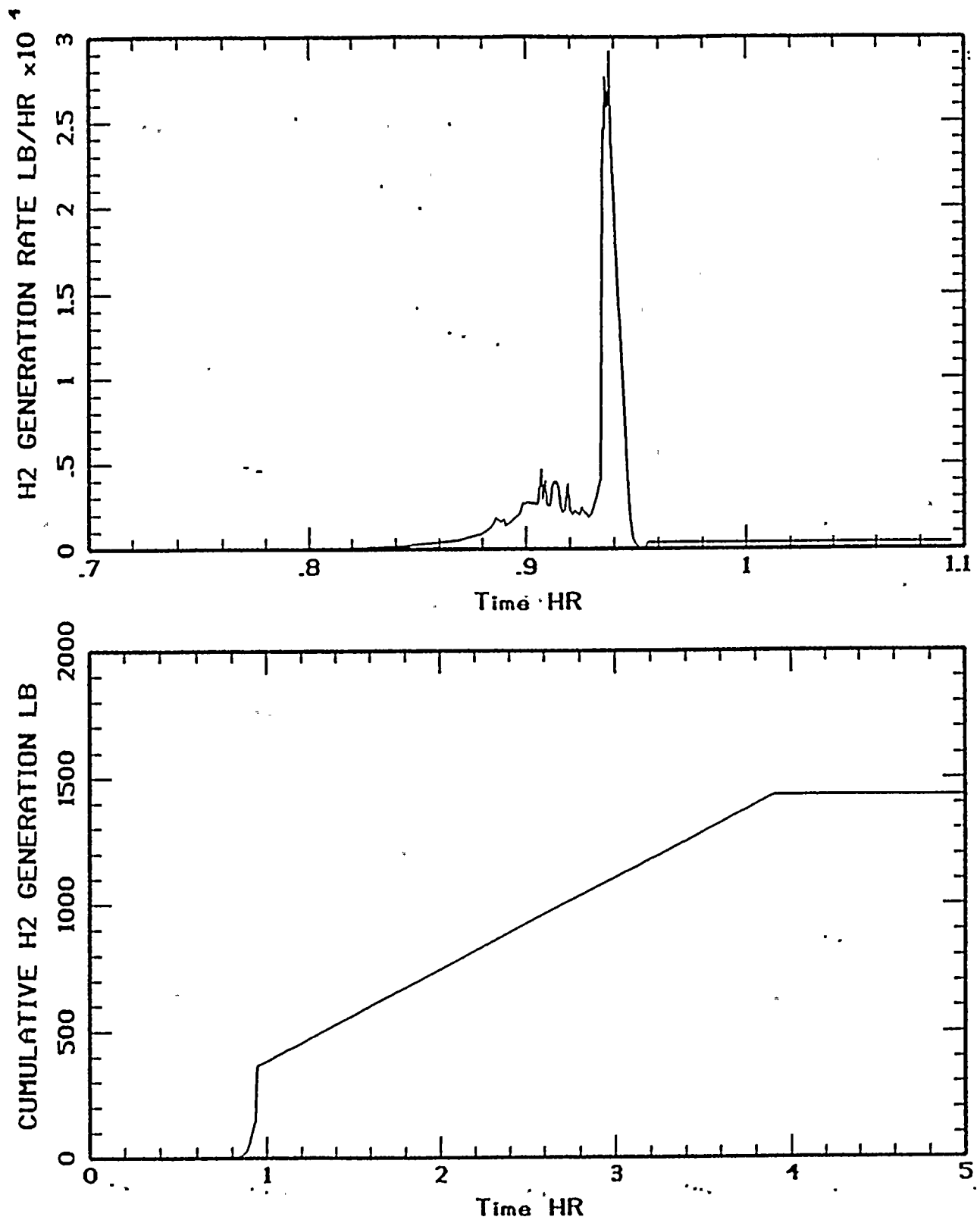


Figure 3.1b Hydrogen generation rate and cumulative hydrogen generation during large LOCA.

soon as core is fully recovered to continue releasing hydrogen into the containment. The non-mechanistic hydrogen generation is terminated when total hydrogen generation reaches 1430 lbm.

The first hydrogen burn occurs in the lower compartment immediately (~ 4 seconds) after reflood initiation when the hydrogen mole fraction in the lower compartment reaches 6.5% while the steam mole fraction is about 11%. After the first burn, the lower compartment is momentarily steam-inerted (with a peak of 76% steam). The steam mole fraction then rapidly decreases to about 30% and gradually to 25% over a 4-hour period until the end of the scenario at 5 hours (Figure 3.1c). The high steam content in the lower compartment raises the upward lean flammability limits in the lower compartment higher than that in the annular compartment where the steam mole fraction is only about 8.5%.

Due to the relatively small amount of clad-water reactions during reflood, no other burns of mechanistically produced hydrogen occur anywhere else. The peak hydrogen mole fraction during reflood neither reaches the ignition criteria in the upper plenum ($\sim 8\%$) nor in the upper compartment ($\sim 6\%$). Further burns occur only in the annular compartment following the addition of non-mechanistic hydrogen into the containment.

In summary, about 160 lbms of mechanistic hydrogen burns in the lower compartment, and about 900 lbms of non-mechanistic hydrogen burns in the annular compartment. The maximum containment pressure due to hydrogen burn in the lower compartment is about 20 psia, and the peak equipment temperature in the lower compartment reaches 234°F (Figure 3.1d).

3.2 Intermediate Pressure Scenario: Small Break LOCA

A small LOCA accident represents an intermediate pressure (~ 1100 psia) scenario where primary system pressure at the time of core recovery is too high for the RHR pumps to deliver any flows. Core recovery must rely on the SI pumps and/or the charging pumps which deliver flows of maximum 550 gpm per pump for the charging pumps and maximum 650 gpm per pump for the SI pumps. In this scenario, the recovery flowrate is about 500 to 550 gpm supplied by one charging pump. In the IPE analysis, failure of high pressure recirculation was found to be more significant than failure of ECCS injection. However, to accelerate core uncover, failure of ECCS injection from RWST to vessel is assumed.

Core Recovery Criteria

This accident scenario is initiated by a 1.767 sq. inch (1.5 inch equivalent diameter) small break LOCA at the cold leg. Recovery of the heated core is delayed resulting in a 50% clad melt fraction. The following ECCS equipment is assumed operational to mitigate the accident and recover the core, and are modeled accordingly in MAAP:



D.C. COOK LARGE LOCA
BASE CASE ANALYSIS

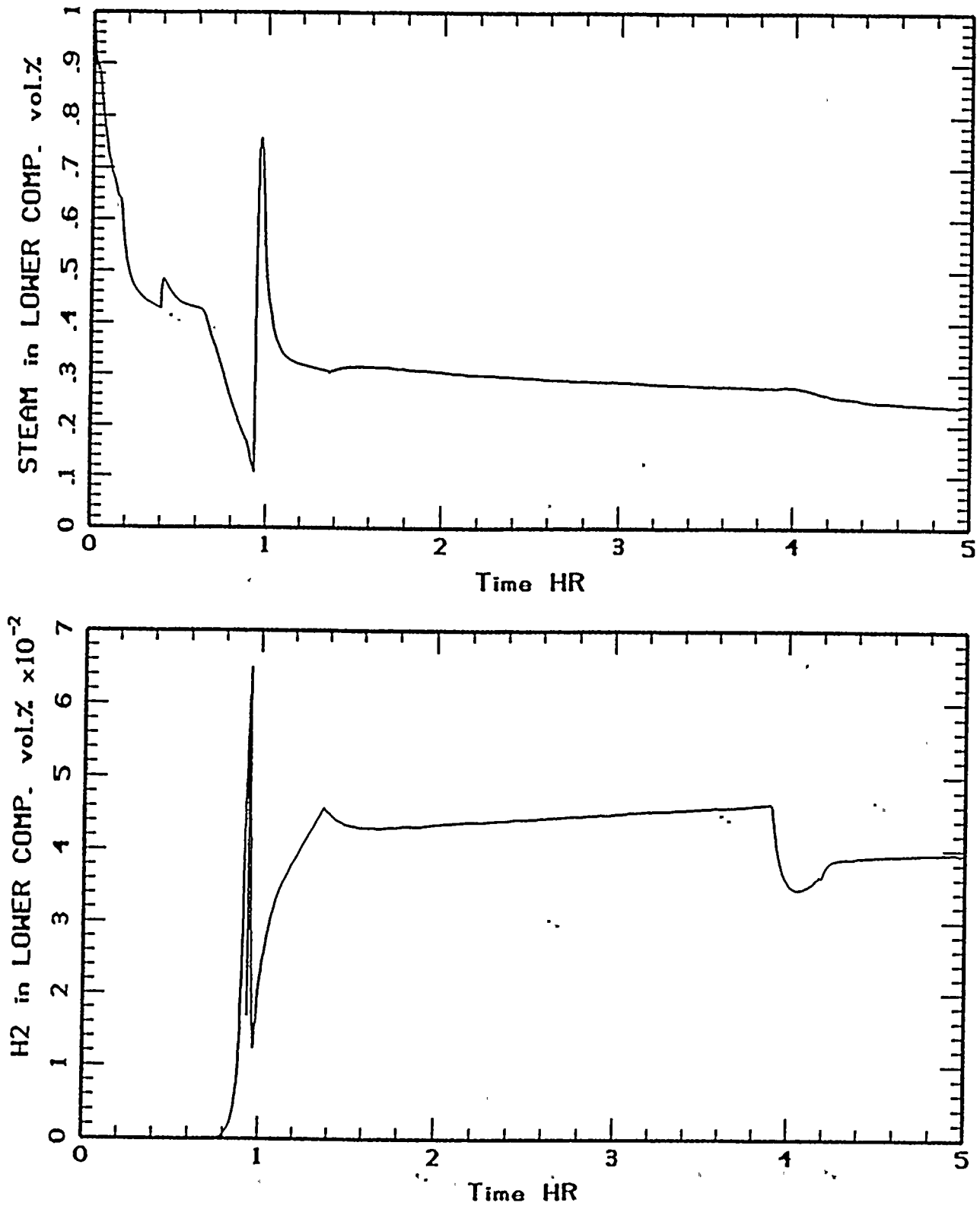


Figure 3.1c Steam and hydrogen concentrations in the lower compartment during large LOCA.

D.C. COOK LARGE LOCA
BASE CASE ANALYSIS

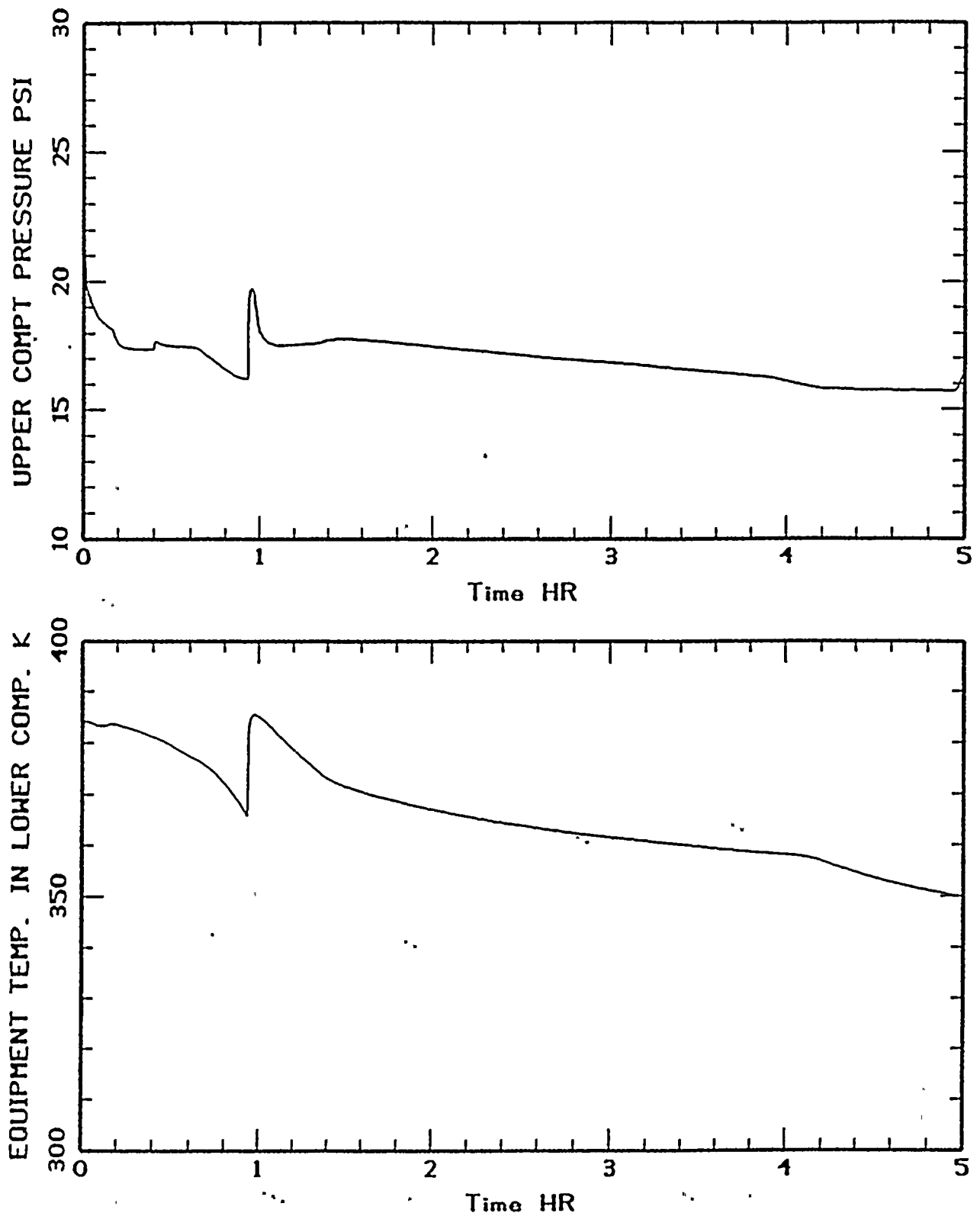


Figure 3.1d Upper compartment pressure and lower compartment equipment temperature during large LOCA.



1. 1 of 2 trains of containment spray injection
2. Successful switch to containment spray recirculation
3. High pressure recirculation using 1 of 2 charging pumps inject from the recirculation sump to 1 of 3 intact cold legs
4. 1 of 2 trains of hydrogen igniters in the upper and lower containment regions
5. 1 of 2 containment recirculation fans
6. Auxiliary feedwater

Accident Scenario Description

The accident scenario begins with a blowdown of primary system inventory into the containment through the small (1.5") cold leg break. The containment pressure peaks to 17.6 psia in 6 minutes and actuates containment sprays and a recirculation fan (with a ten minute delay) to reduce the containment pressure. By 6 minutes into an accident, the primary system pressure drops to ~ 1090 psia and remains at this level as auxiliary feedwater removes decay heat until core uncover occurs. At 0.84 hours RWST low level is reached and the sprays are switched to recirculation modes.

With failure of ECCS injection to vessel, water in the reactor vessel drains out and boils away through the cold leg break, and the core uncovers at 1.84 hours. As water level in the core decreases, the uncovered part of the core heats up and in-vessel hydrogen production due to Zircaloy cladding - steam reactions begins at 1.9 hours. About 21 lbm of hydrogen is produced prior to reflood. The average generation rate before reflood is about 0.012 lb/s. At 2.4 hours ECCS recirculation is recovered, and the operators begin to reflood the reactor vessel with water. By this time about 89% of the core is uncovered. The portion of the uncovered core is assumed not to heat up beyond the melting point of Zircaloy (3447°F) by employing artificially high latent heat of fusion of fuel in the analysis. Hence, during core reflood, cladding-steam reactions are assumed to occur at the maximum temperature limited by the Zircaloy melting point and the original core configuration is assumed intact rendering maximum surface areas and steam flow areas for reactions.

The kinetics of a Zircaloy cladding-steam reaction is so rapid that the factor limiting the reaction rate is the rate at which steam is supplied to the reaction surfaces. This rate depends on the core steaming rate which is proportional to the reflood rate. The reflood rate of this scenario is less than the full flow capacity of one charging pump (550 gpm) due to the elevated primary system pressure (~ 1000 psia) (Figure 3.2a). The peak hydrogen generation rate during reflood is 5.0 lbm/s, while the average rate is about 0.58 lbm/s (Figure 3.2b).

D.C. COOK SMALL LOCA
BASE CASE ANALYSIS

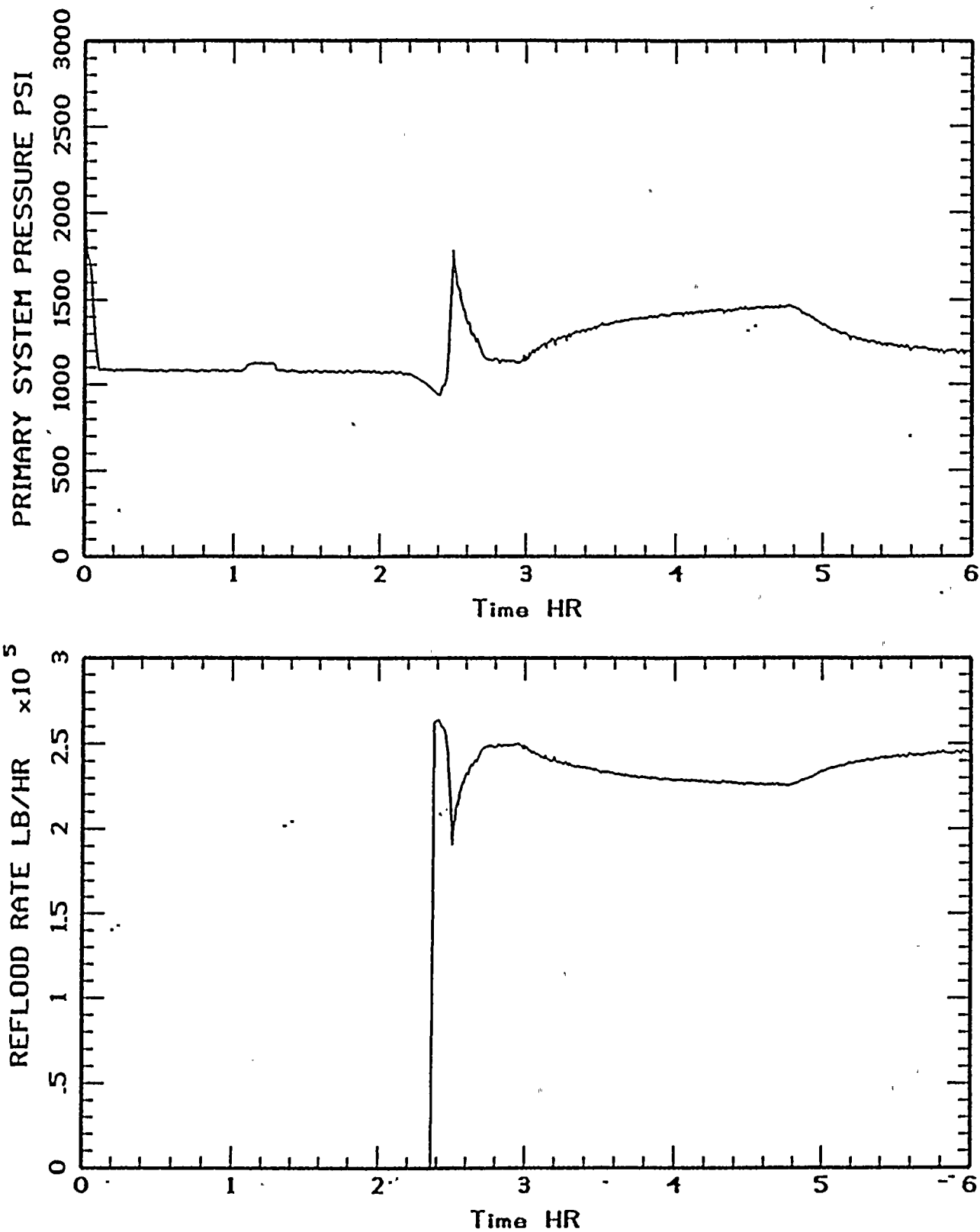


Figure 3.2a Primary system pressure and reflood rate during small LOCA.

D.C. COOK SMALL LOCA
BASE CASE ANALYSIS

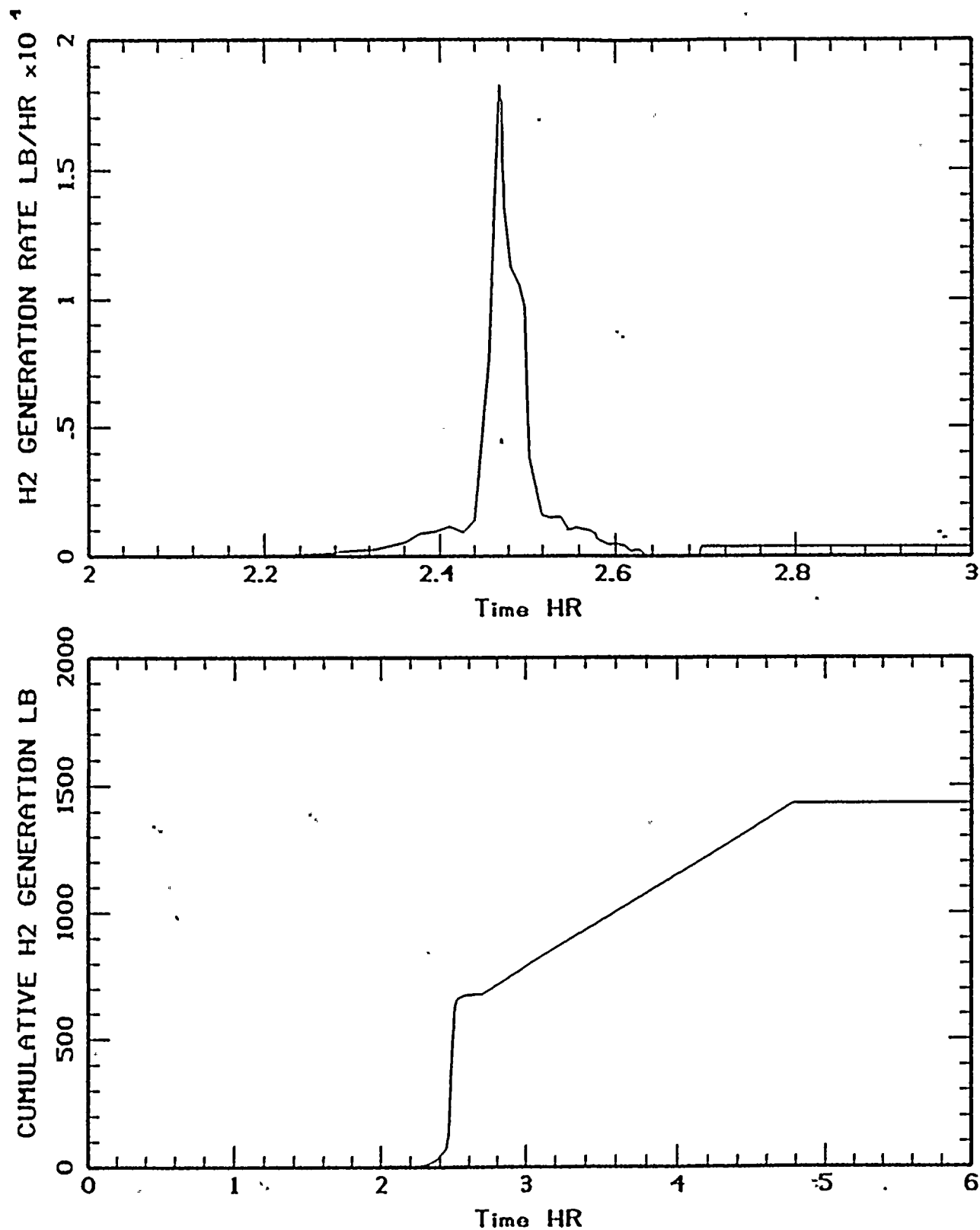


Figure 3.2b Hydrogen generation rate and cumulative hydrogen generation during small LOCA.

Fifteen minutes after reflood initiation, the core is fully recovered with water, terminating further in-vessel clad oxidation. The total in-vessel hydrogen generation until this time is 678 lbm, constituting 35.6% clad-water reactions. To satisfy the 75% clad-water reaction requirement, a non-mechanistic in-vessel hydrogen generation rate of 0.1 lbm/s is assumed as soon as the core is fully recovered to continue releasing hydrogen into the containment. The non-mechanistic hydrogen generation is terminated when total hydrogen generation reaches 1430 lbm.

The first hydrogen burn occurs in the lower compartment a minute after reflood initiation when the hydrogen mole fraction in the lower compartment reaches 6.6% while the steam mole fraction is about 21%. After the first burn, four deflagrations occur in the lower compartment for the next 8 - 9 minutes. The steam mole fraction increases to about 30% during the burns and gradually drops to 18% and then 16% over a 3-hour period until the end of the scenario at 6 hours (Figure 3.2c).

The high steam content in the lower compartment raises the upward lean flammability limits in the lower compartment higher than those in the annular compartment where the steam mole fraction is only about 8.0%. The peak hydrogen mole fraction during reflood neither reaches the ignition criteria in the upper plenum ($\sim 8\%$) nor in the upper compartment ($\sim 6\%$). Hence, following the addition of non-mechanistic hydrogen into the containment, the most likely location to burn is the annular compartment.

From 2.65 hours when non-mechanistic hydrogen generation begins until the end of the sequence at 6 hours, MAAP predicts four deflagrations at $\sim 5.4\%$ H_2 in the lower compartment and, a long continuous series of small deflagrations (at 4.8% H_2) in the annular compartment.

In summary, 220 lbm of mechanistic hydrogen and 120 lbm of non-mechanistic hydrogen burn in the lower compartment. 605 lbms of non-mechanistic hydrogen burns in the annular compartment. The maximum containment pressure of 19.3 psia is caused by the first hydrogen burn in the lower compartment, and the peak equipment temperature in the lower compartment reaches only $192^\circ F$ (Figure 3.2d).

3.3 High Pressure Scenario: Loss of Component Cooling Water Accident

A loss of component cooling water (CCW) accident represents a high primary system pressure scenario in which SI pump capacity is exceeded or not sufficient for core recovery. Core recovery must at least rely on RCS depressurization and a combination of one charging pump and one SI pump. In this scenario, the recovery flowrate is about 400 to 720 gpm supplied by one charging pump and one SI pump. To accelerate core uncover, failure of ECCS injection from RWST to vessel is assumed.



D.C. COOK SMALL LOCA
BASE CASE ANALYSIS

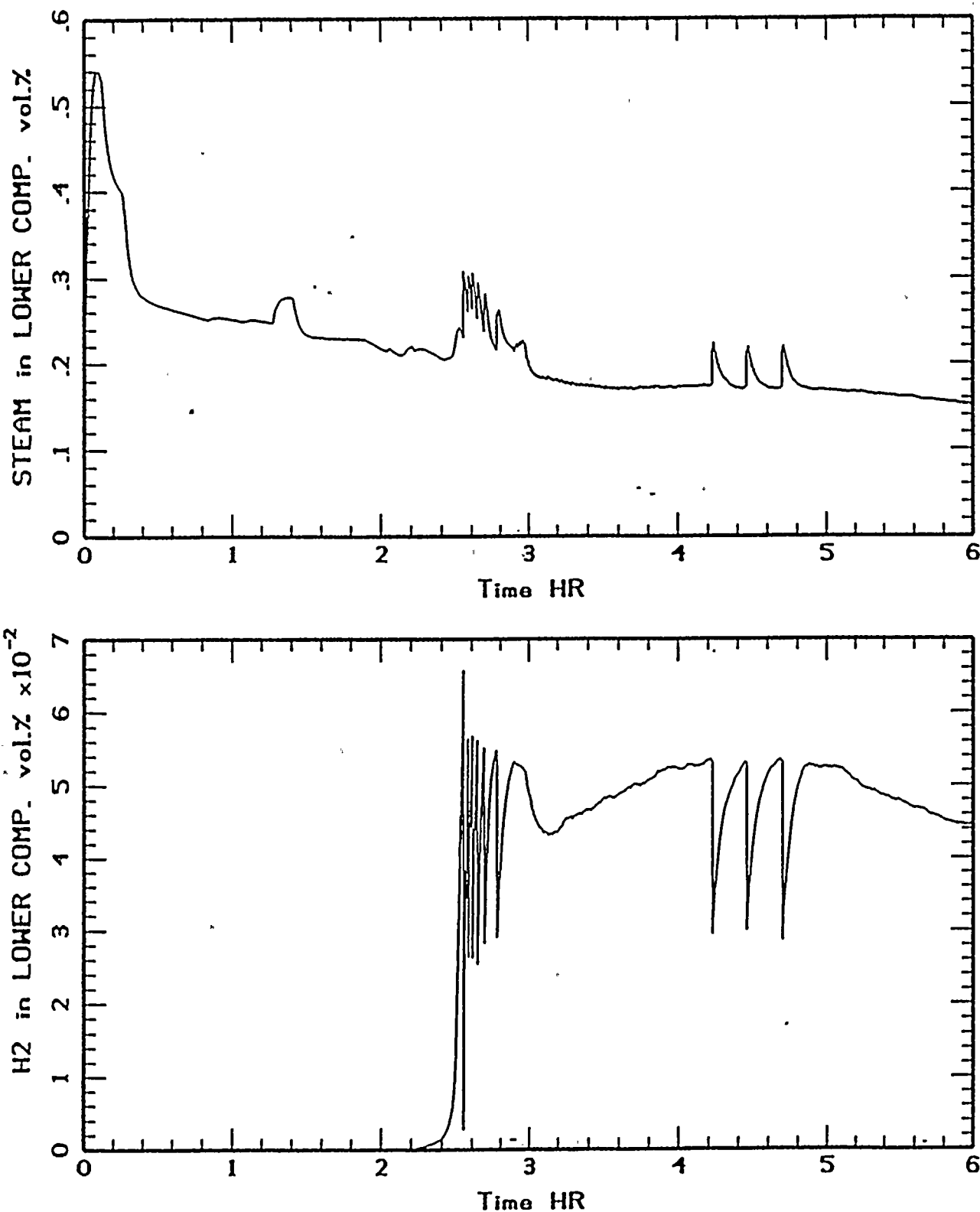


Figure 3.2c Steam and hydrogen concentrations in the lower compartment during small LOCA.

D.C. COOK SMALL LOCA
BASE CASE ANALYSIS

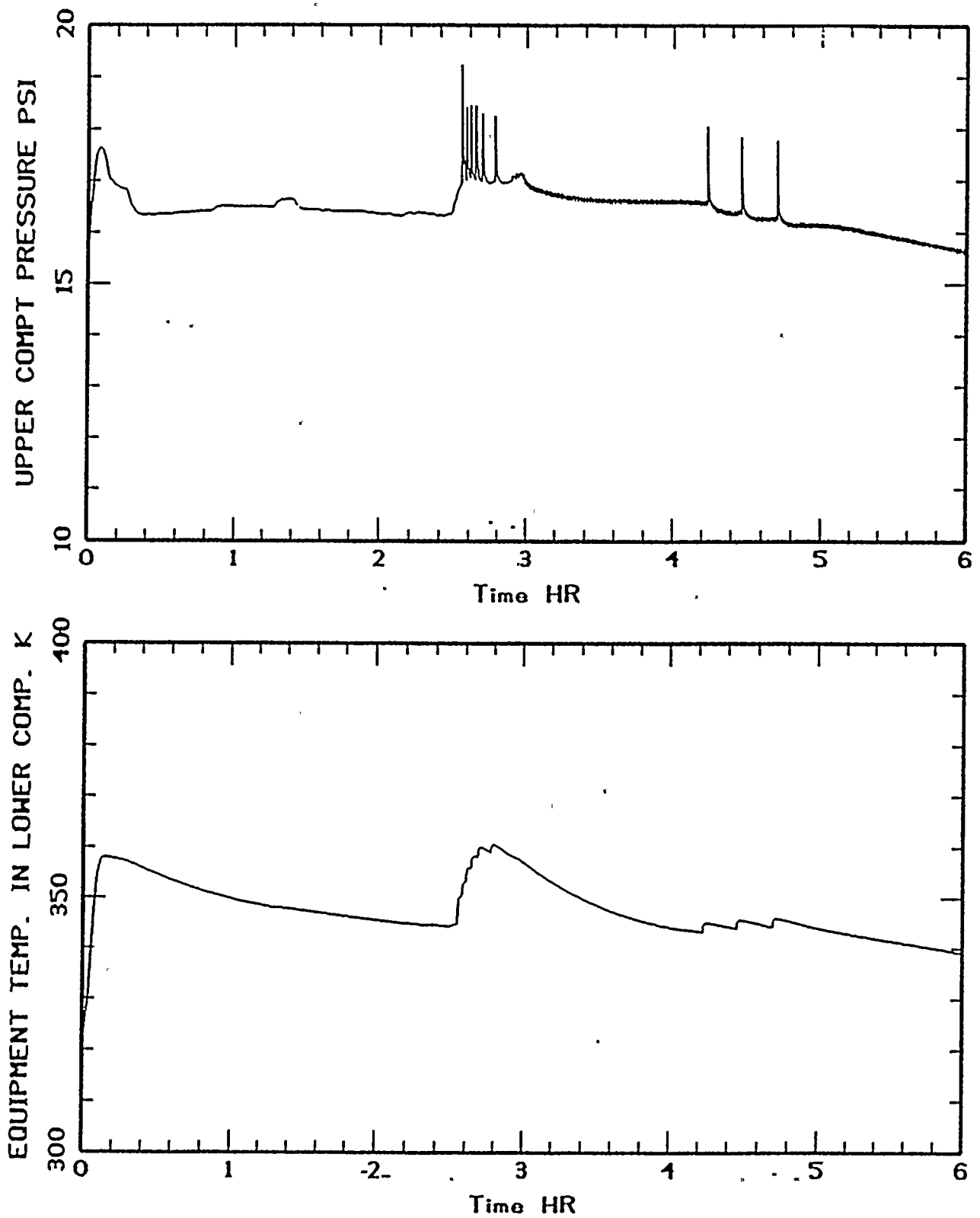


Figure 3.2d Upper compartment pressure and lower compartment equipment temperature during small LOCA.



Core Recovery Criteria

This accident scenario is initiated by a loss of component cooling water resulting in a RCP seal leakage of 21 gpm per pump, and losses of all ECCS injection and containment recirculation fans until restoration of the CCW systems. Restoration of the CCW system is assumed successful within one hour into the accident. Following restoration of the CCW system, the following ECCS equipment is assumed operational to mitigate the accident and eventually recover the core, and are modeled accordingly in MAAP:

1. 1 of 2 trains of containment spray injection
2. Successful switch to containment spray recirculation
3. High pressure recirculation using 1 of 2 charging pumps and 1 of 2 SI pumps inject from the recirculation sump to 1 of 3 intact cold legs at a delayed time resulting in 50% clad melt fraction.
4. Primary system depressurization by manually opening 2 of 3 pressurizer PORVs from the time of high pressure recirculation until the time the core is fully recovered with water.
5. 1 of 2 trains of hydrogen igniters in the upper and lower containment regions
6. 1 of 2 containment recirculation fans

Accident Scenario Description

The accident scenario begins with a loss of primary system water onto the lower compartment floor through the relatively small RCP seal leakage. By 1.2 hours into an accident, the primary system pressure drops to ~ 1720 psia and as the remaining coolant heats up and expands, the primary system pressure rises to the PORV setpoint at 2 hours. The containment pressure rises up slowly to 17.2 psia when CCW is recovered at 1 hour. Upon CCW recovery, the operators actuate containment sprays and a recirculation fan to reduce the containment pressure. At 1.74 hours RWST low level is reached and the sprays are switched to recirculation.

With failure of ECCS injection to vessel, water in the reactor vessel drains out and boils away and the core uncovers at 2.75 hours. As the water level in the core decreases, the uncovered part of the core heats up and in-vessel hydrogen production due to Zircaloy cladding - steam reactions begins at 2.9 hours. About 41 lbm of hydrogen is produced prior to reflood. The average generation rate before reflood is about 0.018 lb/s. At 3:53 hours ECCS recirculation is recovered, and the operators open the pressurizer PORVs and begin to reflood the reactor vessel with water. By this time about 95% of the core is uncovered. The portion of the uncovered core is assumed not to heat up beyond the melting point of Zircaloy (3447°F) by

employing artificially high latent heat of fusion of fuel in the analysis. Hence, during core reflood, cladding-steam reactions are assumed to occur at the maximum temperature limited by the Zircaloy melting point and the original core configuration is assumed intact rendering maximum surface and steam flow areas for reactions.

The kinetics of a Zircaloy cladding-steam reaction is so rapid that the factor limiting the reaction rate is the rate at which steam is supplied to the reaction surfaces. This rate depends on the core steaming rate which is proportional to the reflood rate. The reflood rate of this scenario is limited by the elevated primary system pressure (~ 2350 psia). Initially, the reflood rate is only 280 gpm when the primary system is at ~ 2300 psia. About 5 minutes later, the core is fully uncovered. As steam is released through the PORVs, the primary system pressure decreases and the reflood rate increases to the peak value of 720 gpm. The reflood rate then decreases to 400 gpm as cooling of the heated core causes explosive steaming that increases the primary system pressure to 1800 psia (Figure 3.3a). Similar pressure-reflood rate transients occur several times at different magnitude for the total transient time of about 40 minutes. The peak hydrogen generation rate during reflood is 3.0 lbm/s, while the average rate is about 0.45 lbm/s (Figure 3.3b). The steam pressure transients and calculated maximum amount of Zircaloy-water reactions is undoubtedly exaggerated by the artificial assumptions used to maintain the core integrity. However, these assumptions keep both the rate and mechanistic hydrogen production conservatively high.

Forty minutes after reflood initiation, the operators close the PORVs and the core is fully recovered with water, terminating further in-vessel clad oxidation. The total in-vessel hydrogen generation until this time is 972 lbm, constituting 51.0% clad-water reactions. To satisfy the 75% clad-water reaction requirement, a non-mechanistic in-vessel hydrogen generation rate of 0.1 lbm/s is assumed as soon as the core is fully recovered to continue releasing hydrogen into the containment. Non-mechanistic hydrogen generation is terminated when total hydrogen generation reaches 1430 lbm.

The first hydrogen burn occurs simultaneously in the lower compartment and in the upper plenum fifteen minutes after reflood initiation when the hydrogen mole fraction peaks at 7.7% in the lower compartment and at 8.0% in the upper plenum. After the first burn, there are two more deflagrations in the lower compartment, a 12-minute long continuous series of deflagrations in the upper plenum and, later on, some burning in the annular compartment. Near the end of the mechanistic production period, burning occurs in the upper compartment. This is a consequence of opening the PORVs during reflood that steam releasing from the PORVs keeps the lower compartment inert (40 \sim 50 vol. % steam) for most of the reflood duration (Figure 3.3c). As a result, unburned hydrogen from the lower compartment burns in the upper plenum, in the upper compartment, and in the annular compartment where steam concentrations are much lower.

From 4.19 hours when non-mechanistic hydrogen generation begins until the end of the sequence at 8 hours, MAAP predicts a series of seven small deflagrations in the upper compartment and

D.C. COOL LOSS OF COMPONENT COOLING WATER
BASE CASE ANALYSIS

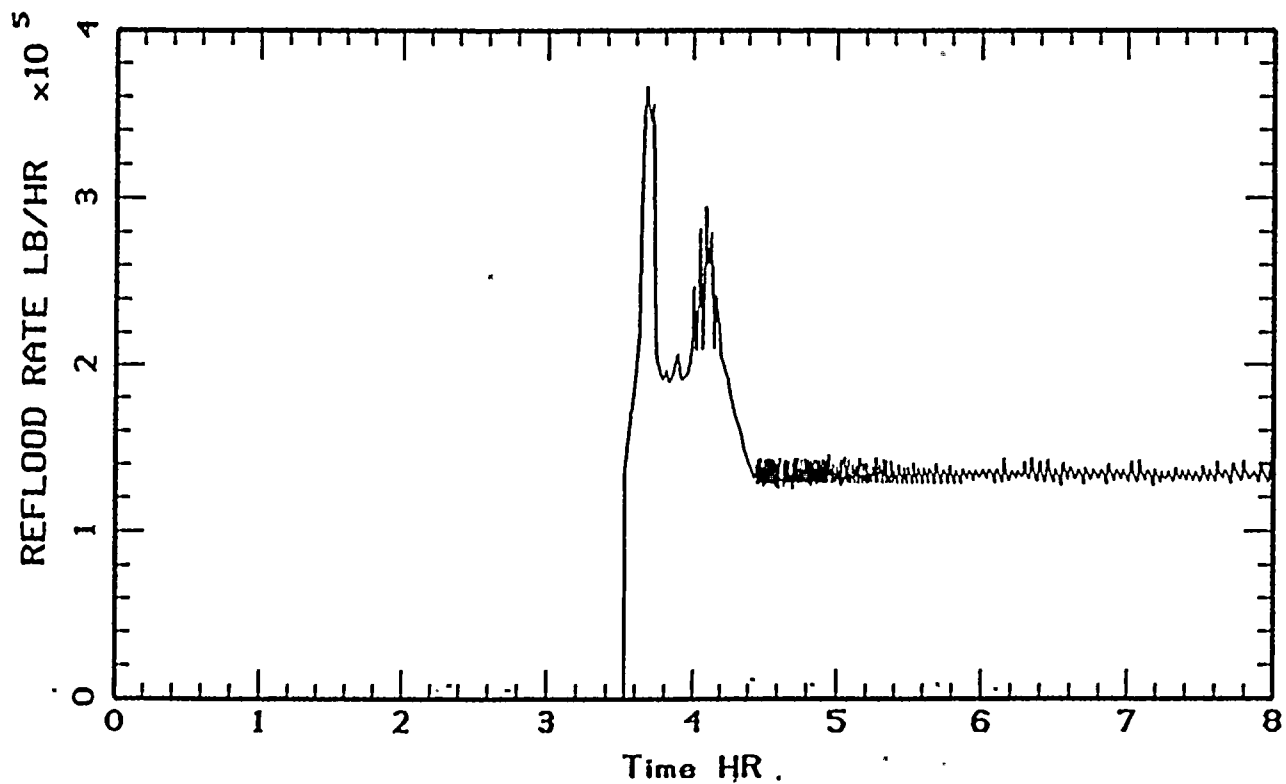
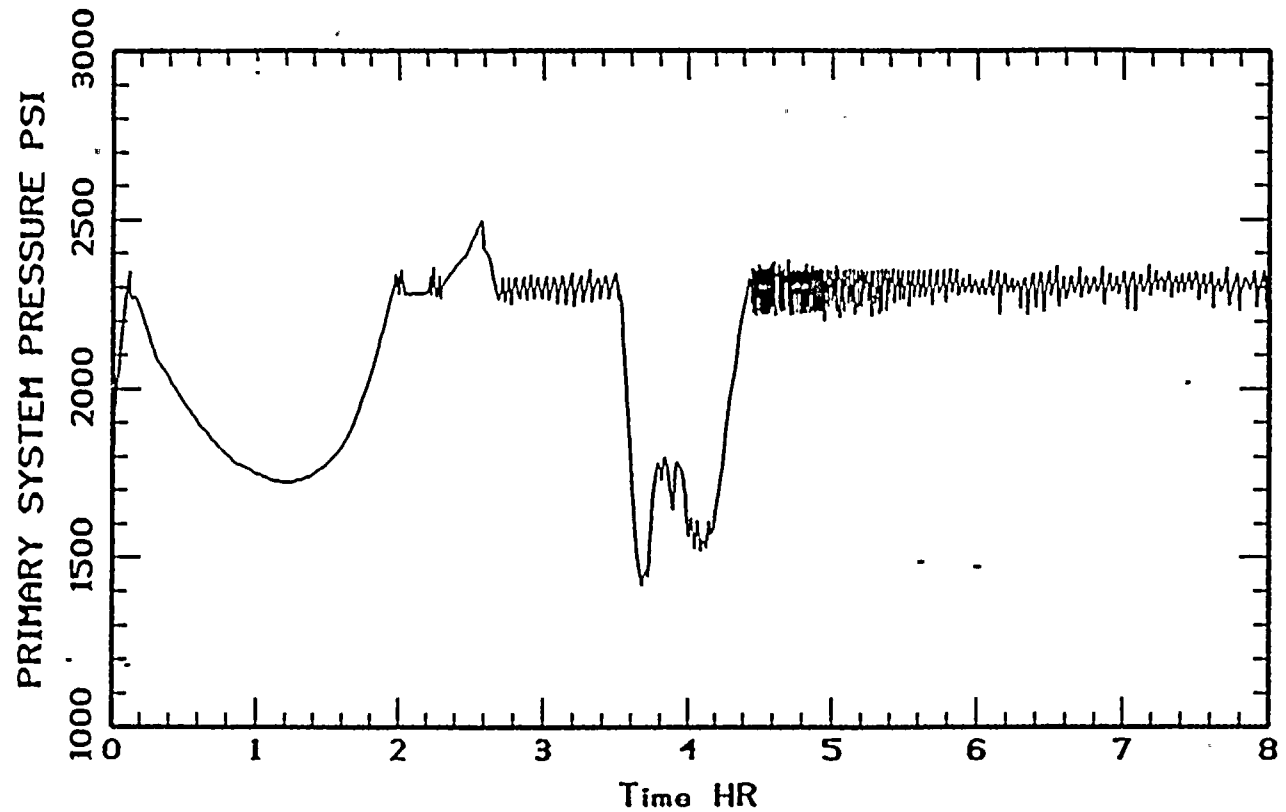


Figure 3.3a Primary system pressure and reflood rate during loss of CCW.

D.C. COOK LOSS OF COMPONENT COOLING WATER
BASE CASE ANALYSIS

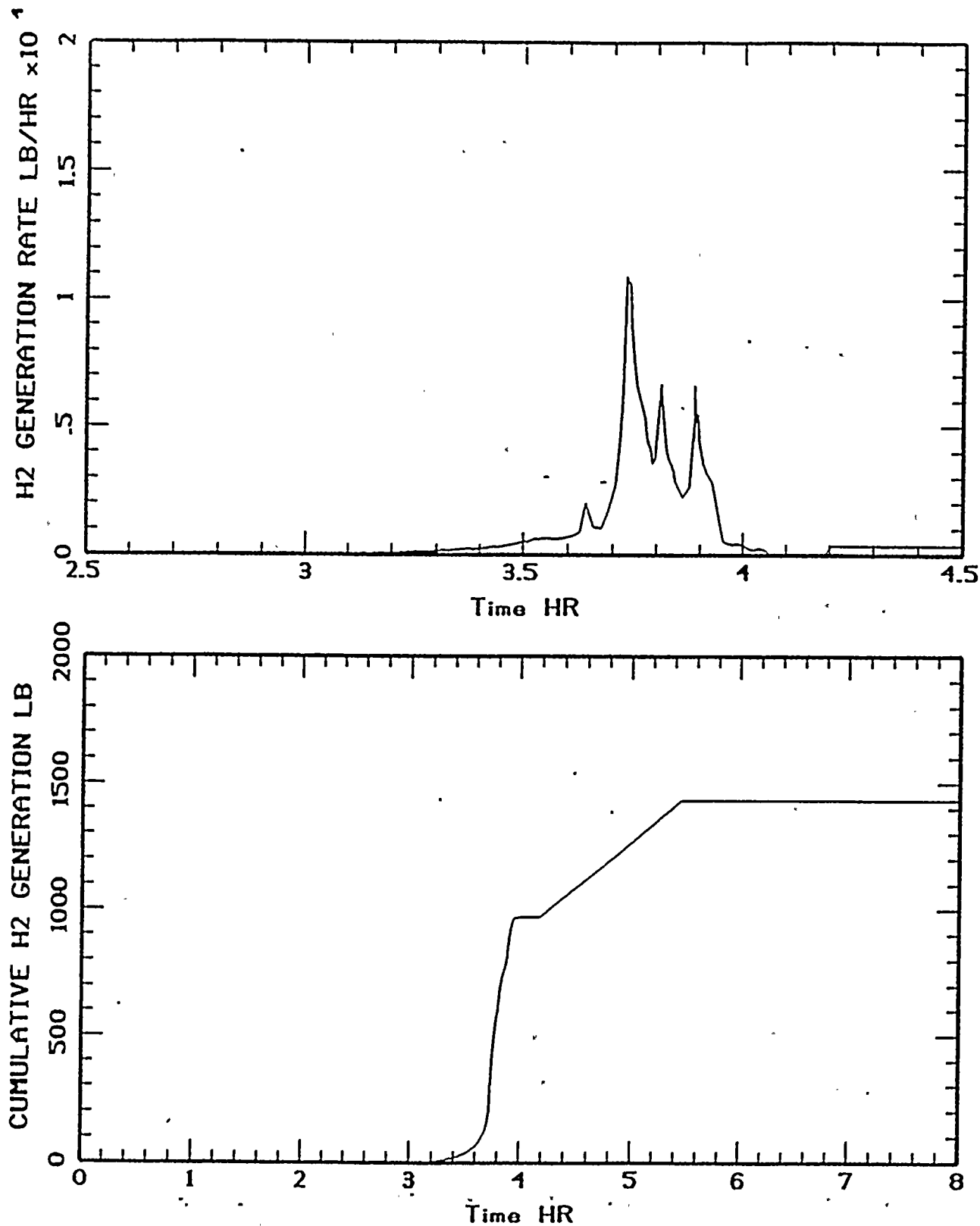


Figure 3.3b Hydrogen generation rate and cumulative hydrogen generation during loss of CCW.

one deflagration in the annular compartment. Due to high steam concentration (20 to 30 vol. %) no burn is observed in the lower compartment during the non-mechanistic hydrogen generation.

In summary, 231 lbm of mechanistic hydrogen burns in the lower compartment, 198 lbms of mechanistic hydrogen burns in the upper plenum, 155 lbm of mechanistic hydrogen burns in the upper compartment, and 44 lbm of mechanistic hydrogen burns in the annular compartment. Most non-mechanistic hydrogen burns in the upper compartment. The maximum containment pressure of 28.0 psia is caused by burning in the upper compartment, and the peak equipment temperature in the lower compartment reaches 217°F (Figure 3.3d).

and one deflagration in the upper compartment and one deflagration in the annular compartment. Due to high concentration (20 to 30 vol. %) no burn is observed in the lower compartment during the non-mechanistic generation.

In summary, 231 lbm of mechanistic hydrogen burns in the lower compartment, 198 lbms of mechanistic hydrogen burns in the upper plenum, 155 lbm of mechanistic hydrogen burns in the upper compartment, and 44 lbm of mechanistic hydrogen burns in the annular compartment. Most non-mechanistic hydrogen burns in the upper compartment. The maximum containment pressure of 28.0 psia is caused by burning in the upper compartment, and the peak equipment temperature in the lower compartment reaches 217°F (Figure 3.3d).

D.C. COOL LOSS OF COMPONENT COOLING WATER
BASE CASE ANALYSIS

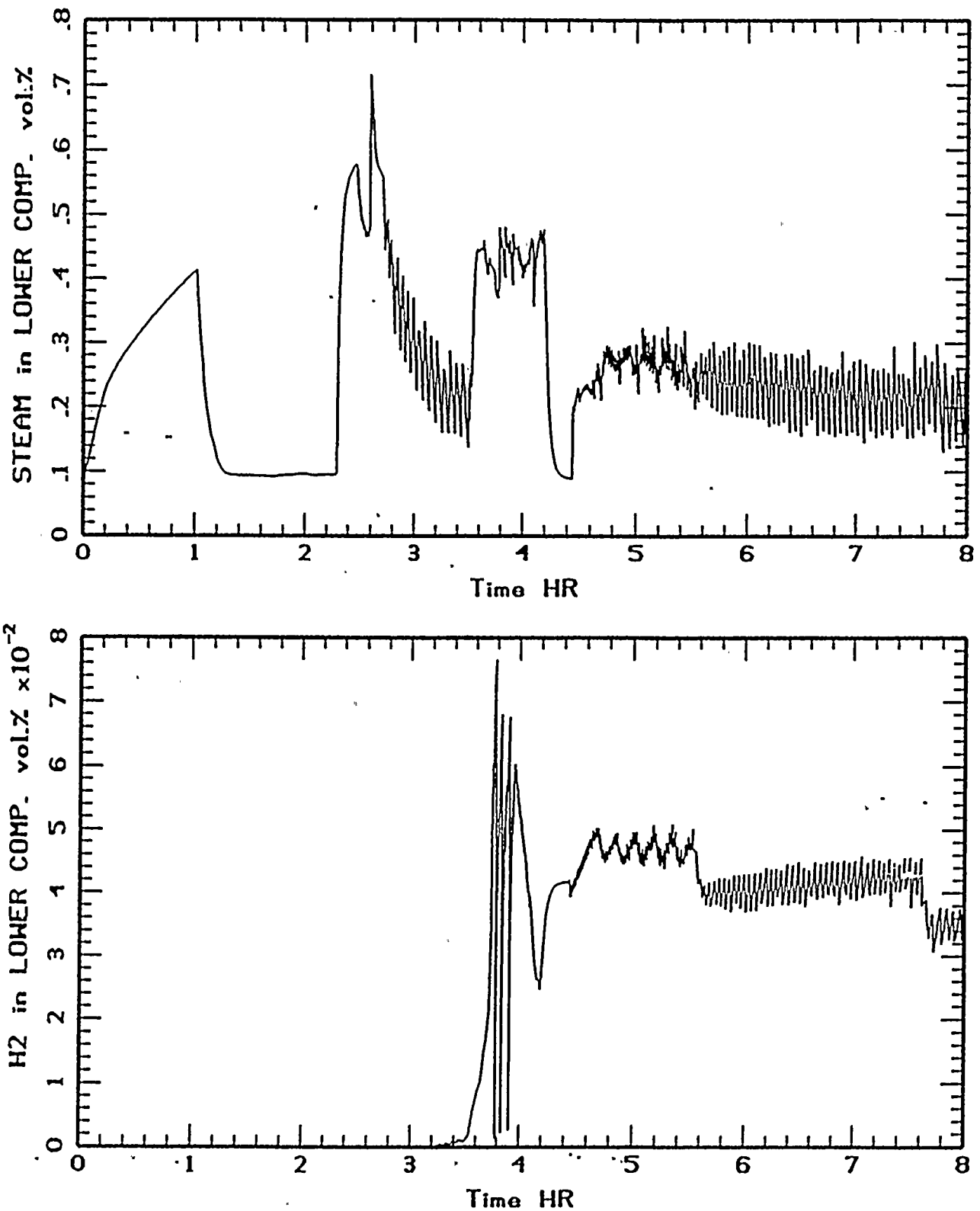


Figure 3.3c Steam and hydrogen concentrations in the lower compartment during loss of component cooling water.

D.C. COOK LOSS OF COMPONENT COOLING WATER
BASE CASE ANALYSIS

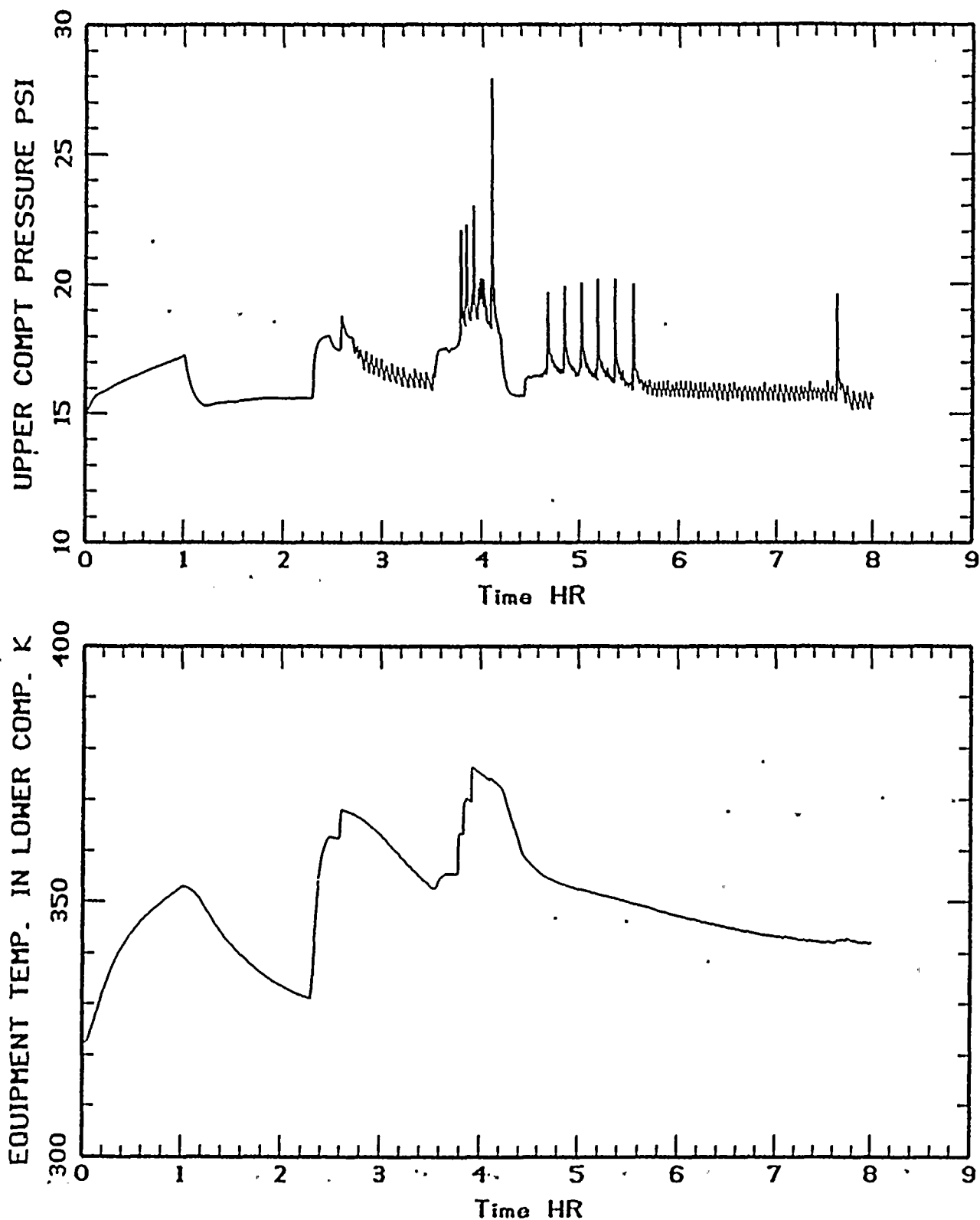


Figure 3.3d Upper compartment pressure and lower compartment equipment temperature during loss of CCW.



4.0

SENSITIVITY ANALYSIS

Combustion phenomena within the reactor containment depend on several modeled parameters. The sensitivity of these parameters on hydrogen generation and on combustion events within their physically realizable range vary in degrees of significance. The base cases presented in Section 3.0 represent a spectrum of scenarios with a wide range of primary system pressure, core reflood rate, hydrogen generation rate and total hydrogen generated mechanistically. All the base cases share the same ignition criteria and the same containment equipments (such as sprays and a recirculation fan).

In this section, sensitivity analysis that may lead to more severe conditions due to hydrogen burning is performed. The parameters to be analyzed include:

- 1) availability of two recirculation fans
- 2) failure of fan, and
- 3) fuel configuration and core power of Unit 2.

In addition, a station blackout scenario is included for analysis to understand the effects of equipment losses for an extended period of time on hydrogen combustion phenomena. Major results of this section can be captured from Table 4-1.

4.1 Two Operating Fans

Purpose

The purpose of this sensitivity analysis, assuming two operating fans available during accident scenarios, is to study effects of early ice depletion on hydrogen combustion events.

Accident Scenario

The accident scenario appropriate for this sensitivity analysis is a large LOCA in which the time between the last burning (after 75% Zircaloy oxidation) anywhere in the containment and the ice depletion time is relatively short. This time duration for the base case large LOCA is about 1 hour.



Table 4-1
D. C. Cook Nuclear Plant 10CFR50.44 MAAP Analysis
Sensitivity Case Summary

Hydrogen Generation and Containment Parameters	Sequences			
	LLO 2 Fans	CCW Fan Failure	LLO Unit 2	SBO
<u>Primary System</u>				
•Core Uncovery Time (hr)	0.62	2.75	0.61	4.96
•Vessel Reflood Time (hr)	0.93	3.53	0.90	5.94
•Pressure @ Reflood (psia)	17	2300	17	1100
<u>H₂ Generation rate (lb/s)</u>				
•Prior to Reflood	0.13	0.018	0.20	0.03
•During Reflood (average/peak)	2.93/8.1	0.45/3.0	3.47/9.2	0.52/5.5
•Artificial "tail"	0.1	0.1	0.1	0.1
Reflood Transient Duration (min)	1.25	40	1.3	26
Reflood Rate (gpm)	4500	400 ~ 720	4500	500
<u>Zr Oxidation (%)</u>				
•Prior to Reflood	7.8	2.2	8.5	3.3
•During Reflood	11.5	48.8	15.5	43.5
•Artificial "tail"	55.7	24.0	51.0	28.2
•Total	75.0	75.0	75.0	75.0
<u>Mass of H₂ Burned (lb)</u>				
•Upper Compartment	---	211*	---	---
•Lower Compartment	160	231	178	770
•Annular Compartment	900	43	798	165
•I/C Upper Plenum	---	506	30	---
<u>Containment Peak Pressure (psia)</u>				
•Upper Compartment	17.6	28	21.5	19.4
<u>Peak Equipment Temperature (°F)</u>				
•Lower Compartment	229	217	242	203

* Fan failure.

MAAP Parameters

For this sensitivity analysis, the number of containment recirculation fans is set to two, all other MAAP parameters remain unchanged from the base case.

Results

With two fans operating during an accident, the forced recirculation flow is doubled resulting in (1) more condensation of steam from the lower containment in the ice bed, (2) faster ice melting rate, and (3) slightly lower containment pressures and temperatures. However, the effects on combustion events are negligible. About the same amount of hydrogen burned at the same locations (lower compartment and annular compartment) and approximately at same time as the base case. Ice depletes at 4 hours about the same time the last hydrogen burning occurs in the annular compartment.

Following ice depletion, containment pressure immediately increases from 16 psia, peaks to 17.6 psia, and stabilizes at about this level for the rest of the sequence which continues for additional three hours.

In conclusion, increasing forced circulation capacity with two fans during an accident would results in negligible differences on the hydrogen combustion events in comparison with the one-fan case. However, the two-fan operation causes earlier ice depletion, but slightly lower gas and equipment temperatures. In either case, the containment integrity is far from being challenged.

4.2 Fan Failure

Purpose

The purpose of this sensitivity case is to identify changes in hydrogen burning rates or locations, and to see if the containment structural capability is challenged, if the containment air recirculation fan fails upon the first burn in upper containment.

Accident Scenario

The accident scenario to be used in this sensitivity analysis will be selected from the base cases where burning occurs in the upper compartment. This leads to the selection of a CCW.

For the base cases, small and large LOCA scenarios do not result in burning in the upper compartment. Peak hydrogen concentrations observed in the upper compartment and in the upper plenum (Figure 4.2a) are summarized below.



D.C. COOK BASE CASES
COMPARISON OF LLO, SLO, CCH

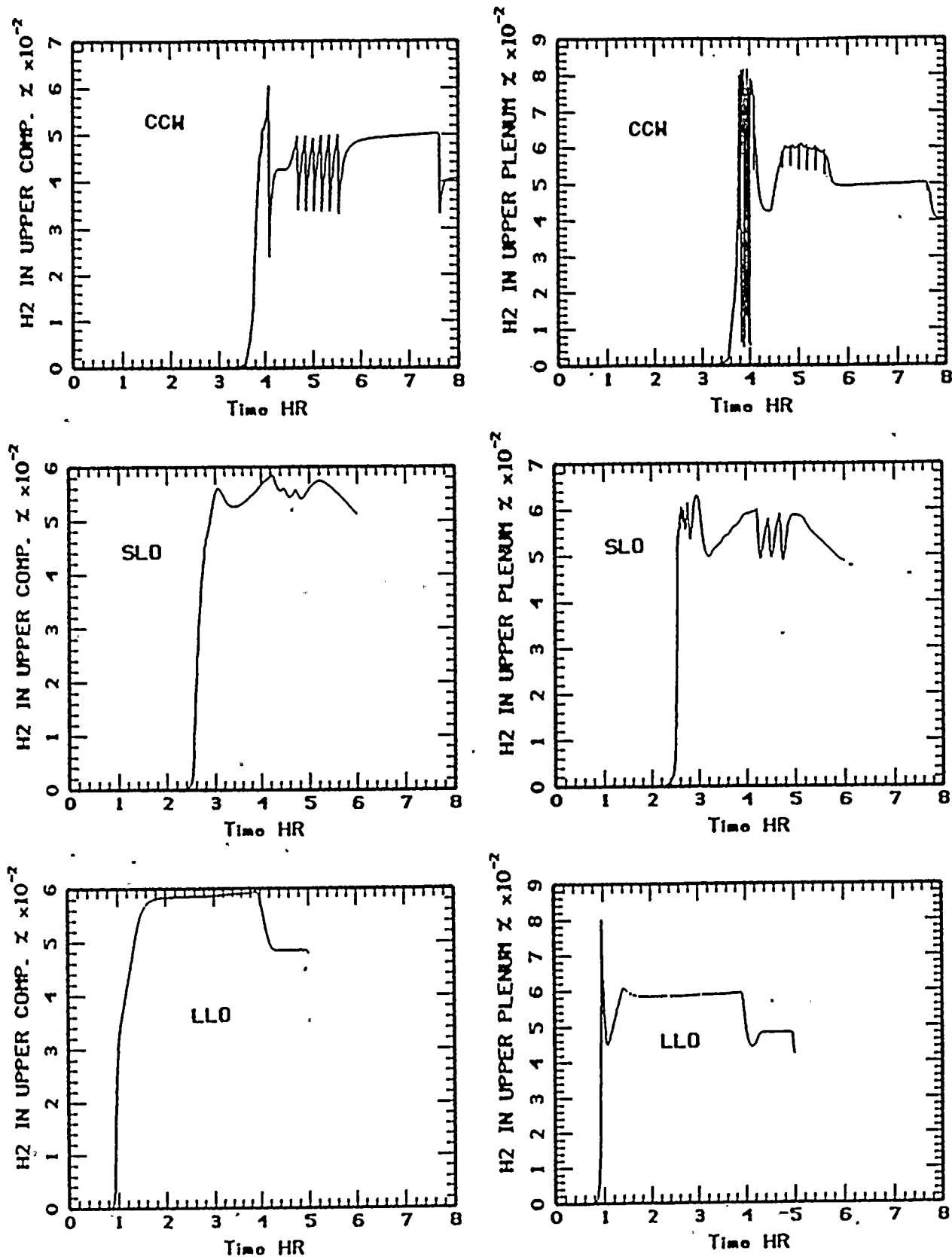


Figure 4.2a Hydrogen concentrations in upper compartment and upper plenum during base cases.



Table 4-2
Base Case Peak H₂ Concentrations

Base Case Accident Scenarios	Peak H ₂ Concentration (vol. %)	
	Upper Compartment (Mechanistic/Artificial)	Upper Plenum (Mechanistic)
Small LOCA	4.6/5.9	6.0
Large LOCA	3.2/5.9	8.0
Loss of component cooling water	6.0/5.0	8.2

The rise of hydrogen concentrations in the upper compartment for small and large LOCA scenarios is attributed to hydrogen added into the containment mechanistically and artificially. The mechanistic portion of peak hydrogen concentrations in the upper compartment for these scenarios are below the normal flammability limit of the upper compartment (expected to be ~ 4.9 vol. % H₂ with ~ 6.5 vol. % steam) with the highest value of 4.6 vol. % H₂ being in the small LOCA, and only 3.2 vol. % H₂ in the large LOCA. The low concentration of 3.2 vol. % H₂ in the large LOCA is due to a short reflood transient duration (~ 1.25 minutes) and a limited mechanistic Zircaloy oxidation (~ 19.3%).

It is noted that in the large LOCA, hydrogen concentration peaks to 8 vol. % but misses the ignition criterion by a fraction of a decimal point. If this conservatism is slightly reduced, burning would occur in the upper plenum for the large LOCA scenario and the mechanistic portion of the peak hydrogen concentration would be less than 3.2 vol. %. Due to an upstream location to the upper compartment, any burning in the upper plenum reduces the amount of hydrogen entering the upper compartment.

In general, accident scenarios (such as the base case CCW) in which a sufficiently large amount of hydrogen is released to the containment during reflood would most likely be susceptible to fan failure due to burning in the upper compartment.



MAAP Parameters

It is conservatively assumed that any hydrogen burning in the upper compartment will result in fan failure regardless of the magnitude of the pressure differential across the fan. The fan area is also reduced to 0.36 ft² to minimize the flow area between the upper compartment and the annular compartment.

Other MAAP parameters are the same as the base case.

Results

Thirty four minutes following reflood, hydrogen burns in the upper compartment at ~ 6 vol. % H₂ resulting in the assumed fan failure. (Accident progression until fan failure occurs is the same as the base case.) The loss of forced recirculation results in a new flow balance based on natural circulation at smaller flow capacity. Due to the reduced capacity the lower compartment gases can be vented to the ice condenser, high steam content (50 to 35 vol.%) in the lower compartment remains until the end of the sequence.

The amount of hydrogen burning in the lower and annular compartments is about the same as the base case. Compared to the base case, hydrogen burns more in the upper plenum and less in the upper compartment (Figure 4.2b). The maximum containment pressure is the same as the base case. The overall effects of fan failure in this scenario is shown to increase more heat load in the upper plenum where burning of non-mechanistic hydrogen occurs continuously for about an hour. The peak temperature of equipment in the lower compartment is the same as the base case, but the non-peak temperatures after fan failure is slightly higher due to the reduced circulation capacity (Figure 4.2c). The peak containment pressure is also the same as the base case. In any case, the large LOCA still predicts a higher equipment temperature.

4.3 Core Power and Fuel Configuration of Unit 2

Purpose

The base case analyses are representative of Unit 1. While the containment designs are identical between Unit 1 and Unit 2 of Cook Nuclear Plant, there are differences in core power and fuel configuration between the two units. The differences in the core design would impact the in-vessel hydrogen generation process. As such, addressing hydrogen generation and combustion events for Unit 2 is the purpose of this sensitivity study.

The differences in the core power and fuel configuration between the two units can be summarized as below.

D.C. COOK LOSS OF COMPONENT COOLING WATER
FAN FAILURE SENSITIVITY ANALYSIS

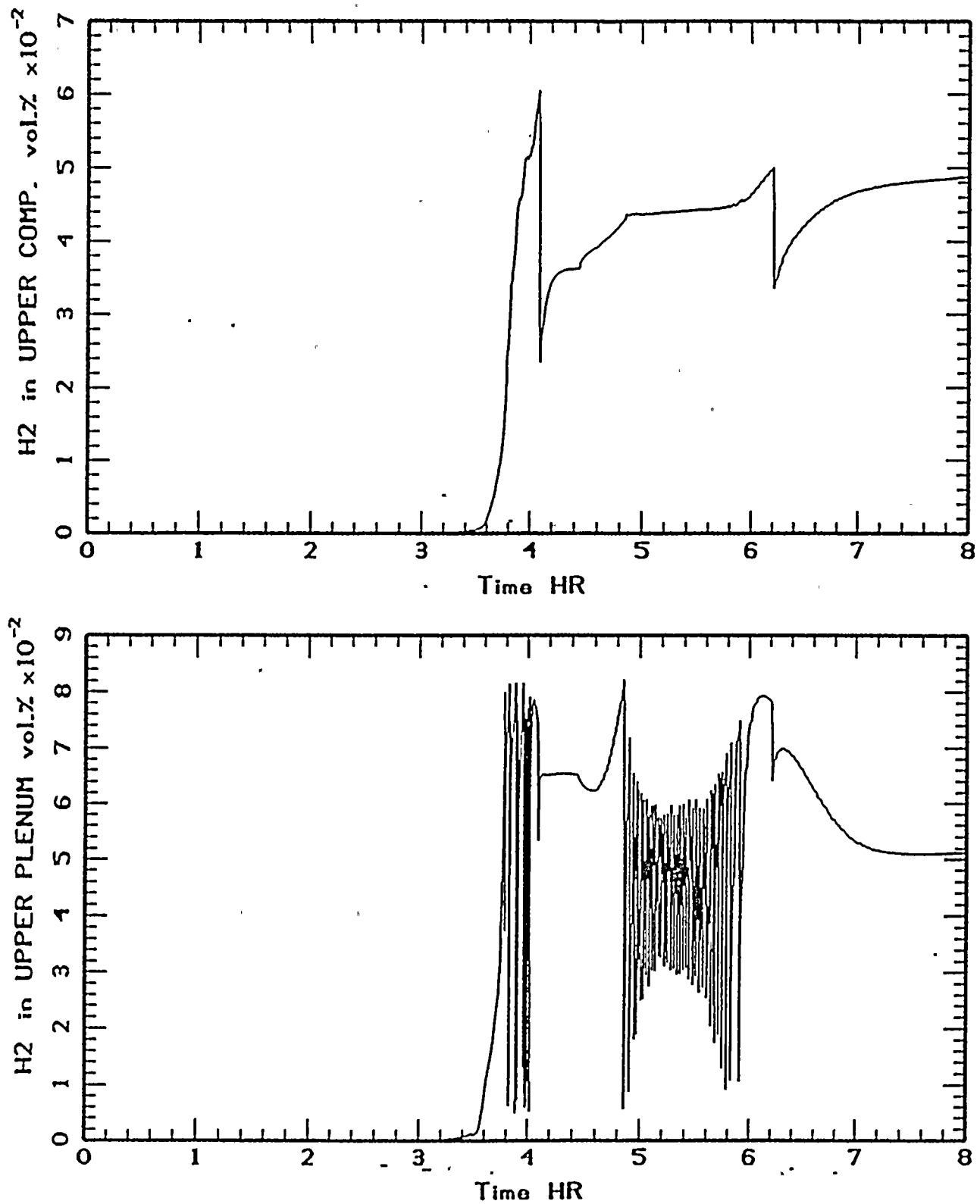


Figure 4.2b Hydrogen concentrations in upper compartment and upper plenum during loss of CCW with recirculation fan failure.

D.C. COOK LOSS OF COMPONENT COOLING WATER
FAN FAILURE SENSITIVITY ANALYSIS

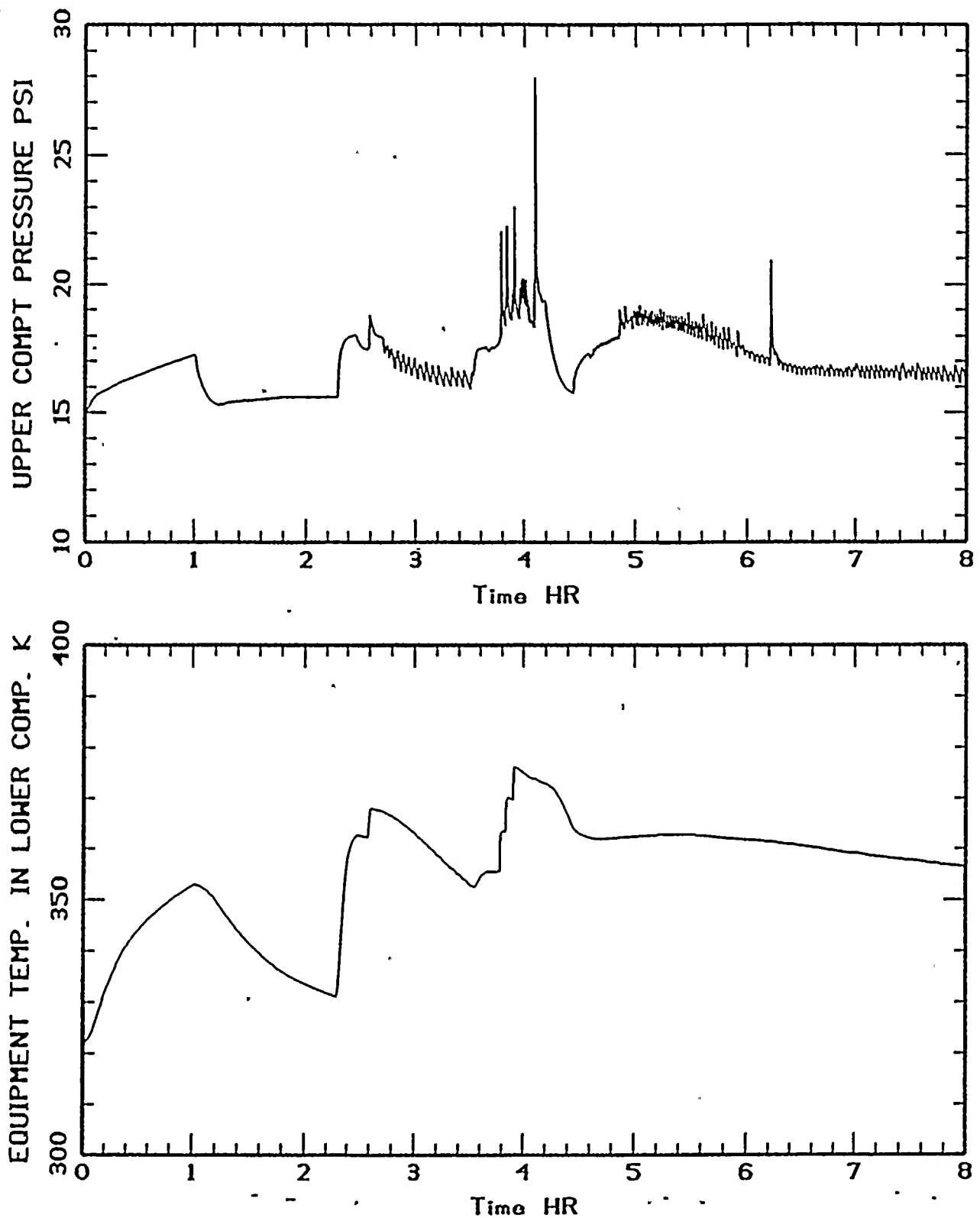


Figure 4.2c Upper compartment pressure and equipment temperature in the lower compartment during loss of component cooling water with fan failure.



Table 4-3
Core Configuration of Unit 1 and Unit 2

Core Parameters	Unit 1	Unit 2
Core power (MWth)	3250	3411
UO ₂ inventory (lbm)	194243	204194
Zircaloy cladding (lbm)	43521.5	39758
Fuel pin outer diameter (ft)	3.517×10^{-2}	3.00×10^{-2}
Number of fuel pin	39372	50952
Fuel pellet radius (ft)	1.524×10^{-2}	1.2867×10^{-2}
Cladding thickness (ft)	2.05×10^{-3}	1.875×10^{-3}
Core flow area + bypass (ft ²)	52.23	54.79

The core of Unit 2 has about 5% more power, 6.2% more surface area of fuel pin, and 5% more core flow area than Unit 1. These parameters, although not significantly different, would result in collective effects that somewhat increase the hydrogen generation rate.

However, there is 8.6% less Zircaloy cladding in Unit 2. Oxidation of 75% of Unit 2 Zircaloy cladding would produce only 1307 lbm of hydrogen (compared to 1430 lbm for Unit 1).

Accident Scenario

In order to present the bounding accident scenario for Unit 2, the worst case scenario of the base cases should be selected for this sensitivity analysis. This selection criterion leads to a large LOCA scenario as the candidate scenario. Among the base cases, the highest heat loads on equipment in the lower compartment appear in a large LOCA due to the release of a large amount of decay energy through primary system blowdown. This equipment is vital to core recovery operations. Since none of the base cases would challenge the containment integrity, the heat loads on equipments in the lower compartment would become the most important indicator of accident severity.

MAAP Parameters

In this sensitivity analysis, core parameters for Unit 2 listed in Table 4-3 are used as MAAP input parameters. Other MAAP parameters are the same as the base case, including core peaking factors which are assumed to be the same as Unit 1. Within the scope of 10CFR50.44 analysis and the "50% clad met fraction" recoverability criterion, the effects of core power profiles are expected to be negligible.

Results

With 5% higher core power, core heatup in Unit 2 is slightly faster than in Unit 1. To satisfy a core recoverability criterion of 50% clad melt fraction, reflood must be initiated about one minute earlier than Unit 1.

During the boildown phase, about 8.5% cladding oxidation occurs at an average of 0.2 lbm H_2 /s. During the reflood phase, additional 15.5% cladding oxidation occurs in a time frame of 1.3 minutes with a peak rate of 9.2 lbm H_2 /s and an average rate of 3.47 lbm H_2 /s (Figure 4.3a).

The total amount of hydrogen produced mechanistically (before and during reflood) is 420 lbm which is 52 lbm more than Unit 1. This additional hydrogen results in burning in the upper plenum as hydrogen concentration exceeds the 8 vol.% H_2 ignition criterion (Figure 4.3b). About 30 lbm of hydrogen burns in the upper plenum, 178 lbm in the lower compartment, and 798 lbm in the annular compartment. The peak equipment temperature in the lower compartment is 242°F (Figure 4.3c). This is about 8°F higher than Unit 1. Containment pressures and temperatures are slightly higher in Unit 2. The containment pressure peaks to 21.5 psia due to burning in the lower compartment and in the upper plenum during reflood. Ice depletion occurs at 4.6 hours, about 24 minutes earlier than Unit 1.

4.4 Station Blackout

Purpose

To demonstrate the loss of safety equipment for a long period of time on core recovery and hydrogen combustion, a station blackout accident is chosen. This accident is initiated by a loss of offsite AC power accompanied by the loss of the onsite emergency AC power distribution system; critical safety and support systems which rely on AC power are not available until power is restored. Power restoration is assumed at 4 hours into the accident. A RCP seal leakage of 0.133 sq. inch (~ 127 gpm) per pump and operation of turbine-driven auxiliary feed water during the 4-hour blackout are assumed. To accelerate core uncover, failure of ECCS injection from RWST to vessel is assumed following power recovery. Ignition criteria are the same as other base case scenarios.

D.C. COOK LARGE LOCA
UNIT2 SENSITIVITY ANALYSIS

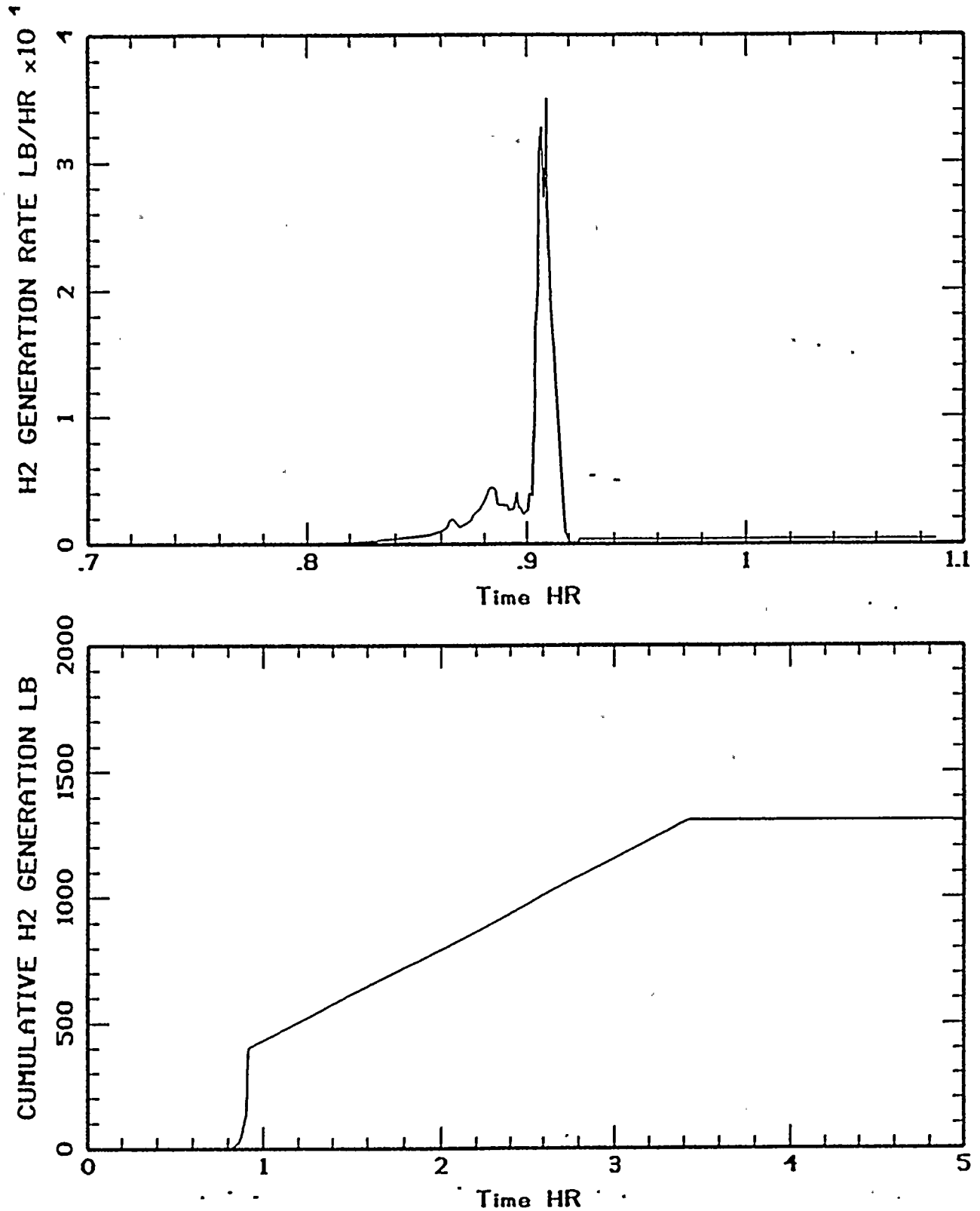


Figure 4.3a Hydrogen generation rate and cumulative hydrogen generation during Unit 2 large LOCA.

D.C. COOK LARGE LOCA
UNIT 2 SENSITIVITY ANALYSIS

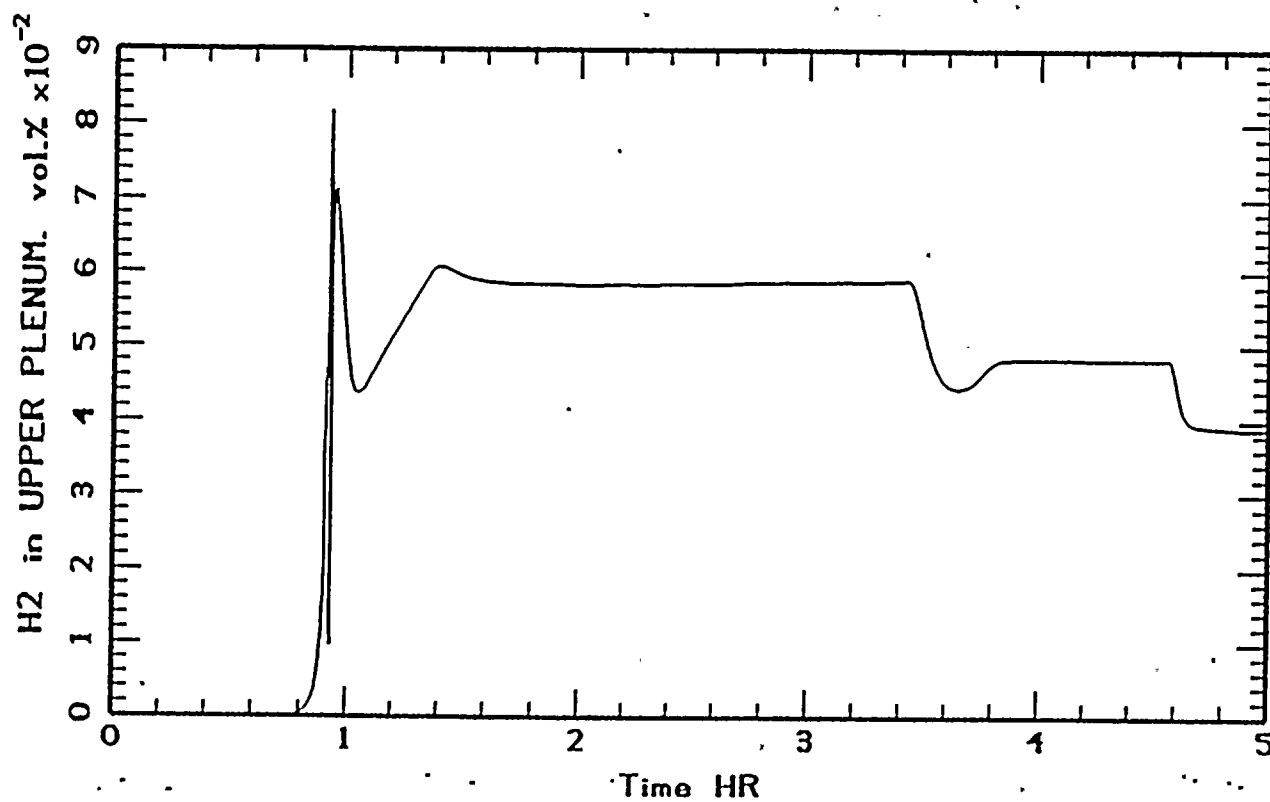
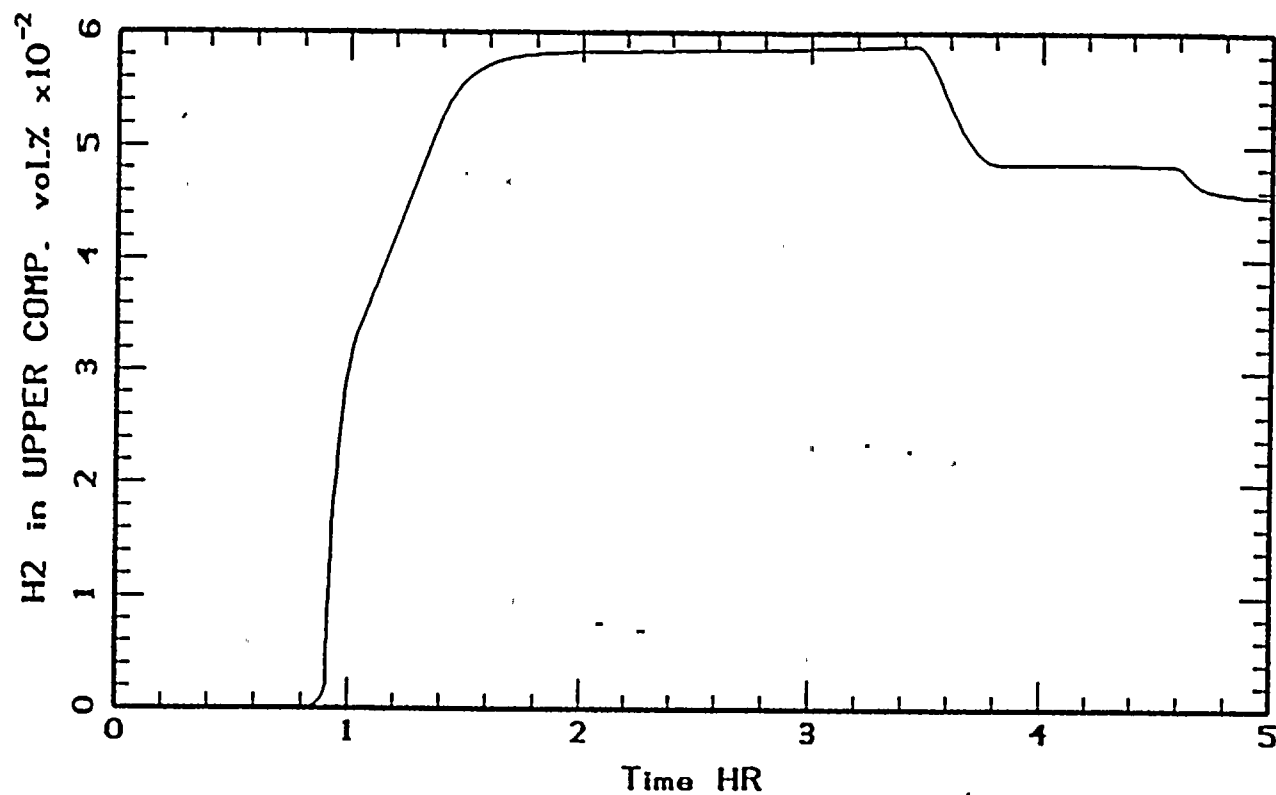


Figure 4.3b Hydrogen concentrations in upper compartment and upper plenum during Unit 2 large LOCA.

D.C. COOK LARGE LOCA
UNIT 2 SENSITIVITY ANALYSIS

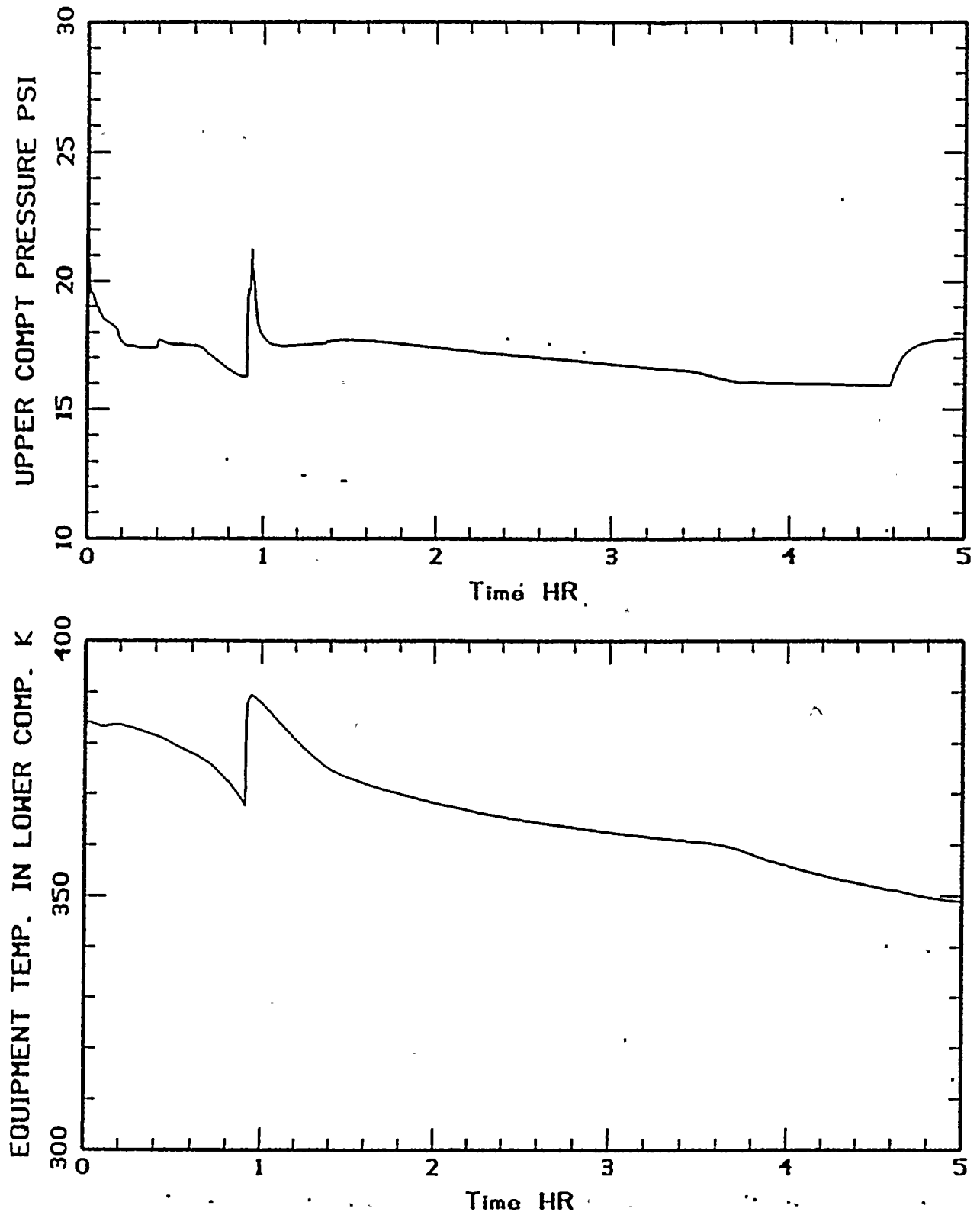


Figure 4.3c Upper compartment pressure and equipment temperature in lower compartment during Unit 2 large LOCA.

Core Recovery Criteria

Following power restoration, the following ECCS equipment is assumed operational to mitigate the accident and eventually recover the core, and are modeled accordingly in MAAP:

1. 1 of 2 trains of containment spray injection
2. Successful switch to containment spray recirculation
3. High pressure recirculation using 1 of 2 charging pumps inject from the recirculation sump to 1 of 3 intact cold legs at a delayed time resulting in 50% clad melt fraction
4. 1 of 2 trains of hydrogen igniters in the upper and lower containment regions
5. 1 of 2 containment recirculation fans
6. Auxiliary feedwater

Results

The accident scenario begins with a loss of primary system inventory into the containment through small ($0.133 \text{ in}^2/\text{pump}$) RCP seal leakage. By 19 minutes into an accident, the primary system pressure quickly drops to $\sim 1160 \text{ psia}$ and remains approximately at this level as auxiliary feedwater removes decay heat until core uncover occurs. The containment pressure peaks to 17.4 psia in about 13 minutes. Later on, the establishment of global natural circulation within the containment, which results in transport of steam from the lower compartment into the ice condenser, adequately maintains the containment pressure in the range of 17 psia until power is recovered at 4 hours.

When power is recovered containment sprays and a recirculation fan are manually actuated, but ECCS injection is assumed failed. With the failure of ECCS injection into the vessel, water in the reactor vessel that has drained out and boiled away through the RCP seal leakage eventually leads to core uncover at 4.96 hours. As the water level in the core decreases, the uncovered part of the core heats up and in-vessel hydrogen production due to Zircaloy cladding - steam reactions begins at 5.33 hours. About 63 lbm of hydrogen is produced prior to reflood. The average generation rate before reflood is about 0.03 lb/s . At 5.94 hours ECCS recirculation is recovered, and the operators begin to reflood the reactor vessel with water. By this time about 87% of the core is uncovered. The portion of the uncovered core is assumed not to heat up beyond the melting point of Zircaloy (3447°F) by employing artificially high latent heat of fusion of fuel in the analysis. Hence, during core reflood, cladding-steam reactions are assumed to occur at the maximum temperature limited by the Zircaloy melting point and the original core configuration is assumed intact rendering maximum surface and steam flow areas for reactions.



The kinetics of a Zircaloy cladding-steam reaction is so rapid that the factor limiting the reaction rate is the rate at which steam is supplied to the reaction surfaces. This rate depends on the core steam rate which is proportional to the reflood rate. The reflood rate of this scenario is less than the full flow capacity of one charging pump (550 gpm) due to the elevated primary pressure (~ 1100 psia). The reflood rate is 500 gpm initially. The reflood rate decreases as cooling of the heated core causes explosive steaming that increases the primary system pressure. The primary system pressure at time of reflood is 1100 psia. Following initial reflood of 500 gpm, the primary system pressure immediately peaks to 2080 psia. The peak hydrogen generation rate during reflood is 5.5 lbm/s, while the average rate is about 0.52 lbm/s (Figure 4.4a).

Twenty six minutes after reflood initiation, the core is fully recovered with water, terminating further in-vessel clad oxidation. The total in-vessel hydrogen generation until this time is 893 lbm, constituting 46.8% clad-water reactions. To satisfy the 75% clad-water reaction requirement, a non-mechanistic in-vessel hydrogen generation rate of 0.1 lbm/s is assumed as soon as the core is fully recovered to continue releasing hydrogen into the containment. The non-mechanistic hydrogen generation is terminated at 7.9 hours when total hydrogen generation reaches 1430 lbm.

The first hydrogen burn occurs simultaneously in the lower and annular compartments. A long elapsed time after core reflood is required prior to the first burn is due to the slow rate of releasing in-vessel hydrogen into the containment. In this scenario only small RCP seal leakage areas serve as an opening from the vessel to the containment.

The steam content ($\sim 12\%$ H_2O) in the lower compartment after the first burn is not much higher than those in the annular compartment (about 6.6%). The peak hydrogen mole fraction neither reaches the ignition criteria in the upper plenum ($\sim 8\%$) nor in the upper compartment ($\sim 6\%$). Hence, following sufficient release of hydrogen into the containment, the most likely locations to burn are both the lower compartment and the annular compartment.

From 6.38 hours when non-mechanistic hydrogen generation begins until the end of the sequence at 13 hours, MAAP predicts a long continuous series of small deflagrations at $\sim 5.5\%$ H_2 in the lower compartment as well as a long continuous series of small deflagrations (at 4.9% H_2) in the annular compartment.

In summary, 770 lbm of hydrogen burns in the lower compartment and, 165 lbms of hydrogen burns in the annular compartment. The maximum containment pressure of 19.4 psia is caused by the first hydrogen burn in the lower compartment, and the peak equipment temperature in the lower compartment reaches 203°F (Figure 4.4b).

D.C. COOK STATION BLACKOUT
BASE CASE ANALYSIS

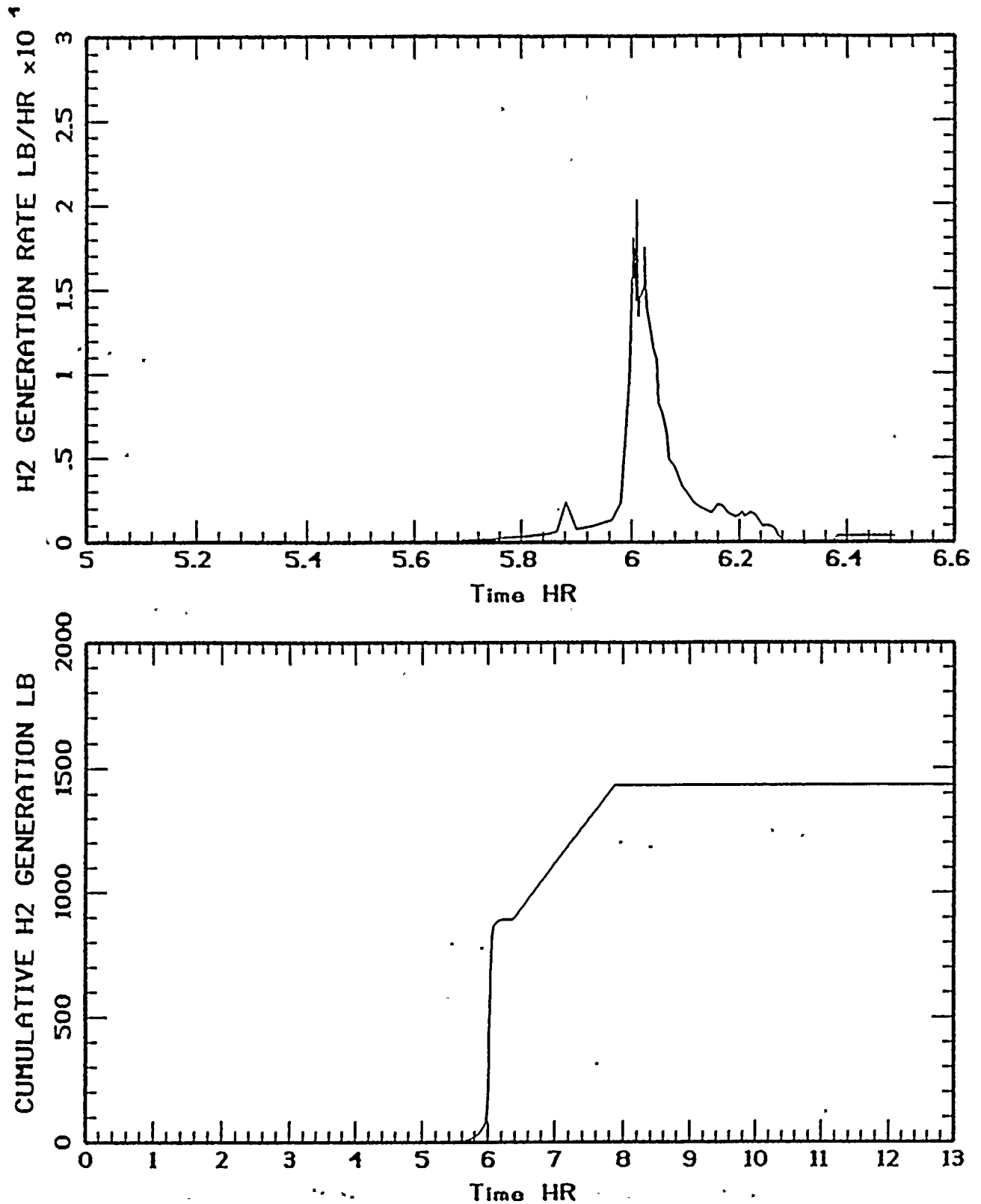


Figure 4.4a Hydrogen generation rate and cumulative hydrogen generation during station blackout.

D.C. COOK STATION BLACKOUT
BASE CASE ANALYSIS

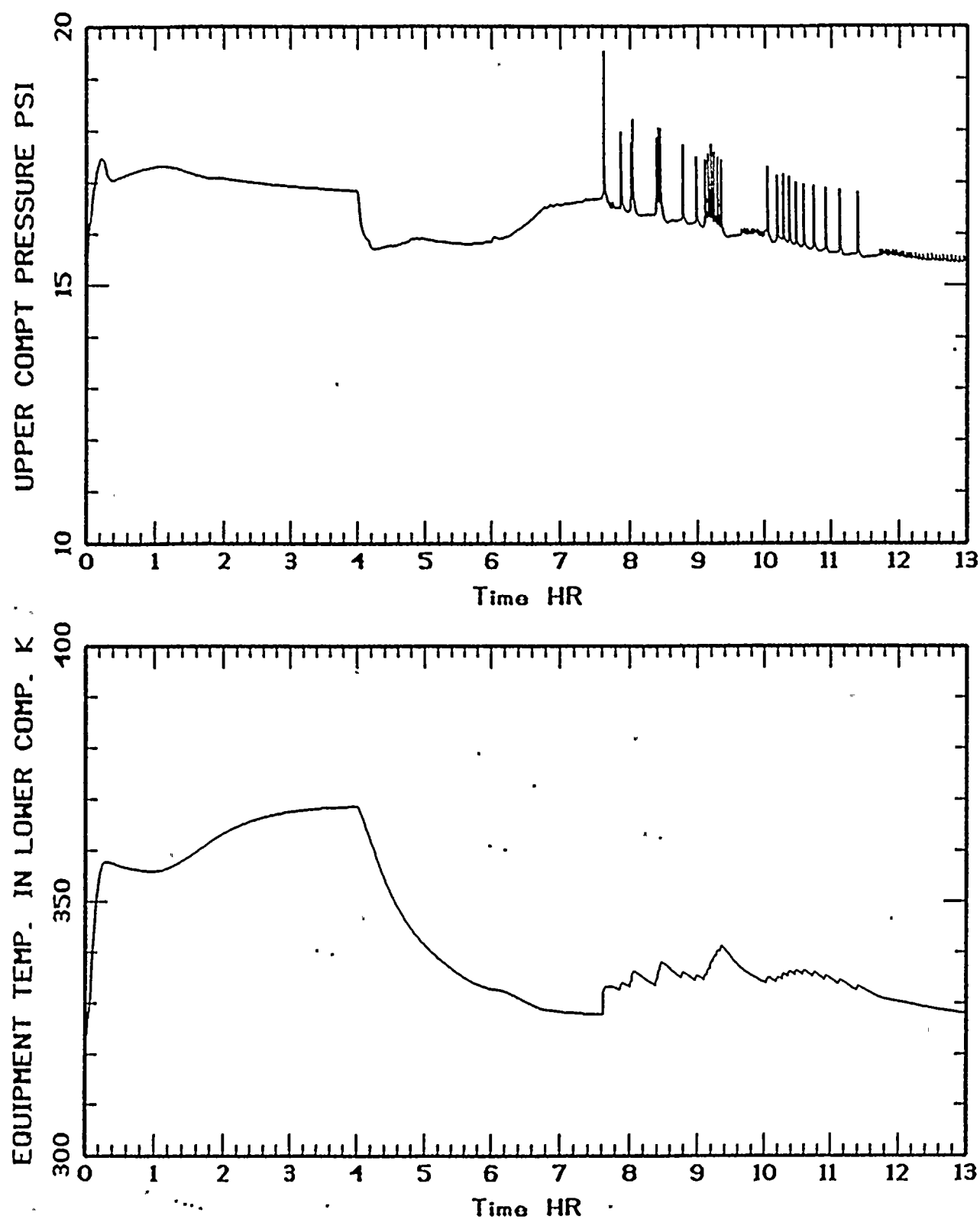


Figure 4.4b Upper compartment pressure and lower compartment equipment temperature during station blackout.

5.0 SUMMARY AND CONCLUSIONS

To demonstrate compliance with 10CFR50.44 for the Cook Nuclear Plant, analyses of accident scenarios with a broad spectrum of hydrogen generation and combustion events are performed. The analyses are performed using MAAP 3.0B with some modifications on combustion models made specifically for the 10CFR50.44 purpose. Three accidents including large break LOCA, small break LOCA, and loss of component cooling water accident, are selected to represent low, intermediate and high pressure scenarios. These sequences were selected based on the Cook Nuclear Plant IPE analysis. In addition, sensitivity analyses are performed to identify potentially more severe conditions than predicted by the base cases. The effects of operating with two recirculation fans, fan failure, fuel configuration and core power of Unit 2, and station blackout are included in the sensitivity analyses.

In this study, core reflood rate ranges from 400 gpm to 4500 gpm, reflood transient time ranges from 1.25 minutes to 40 minutes, and average hydrogen generation rate during reflood ranges from 0.45 lbm H_2 /s to 3.47 lbm H_2 /s. The primary system pressure at time of reflood ranges from 17 psia to 2300 psia.

In any accident scenarios, prediction of in-vessel hydrogen generation by a mechanistic model never exceed the 75% clad-water reaction 10CFR50.44 requirement. To satisfy the requirement, a mechanistic hydrogen production is maximized through the use of "50% clad melt fraction" recoverability criterion. In this criterion, cladding oxidation is assumed to occur at the maximum temperature limited by the Zircaloy melting point, and the original core configuration is assumed intact rendering maximum surface areas and steam flow areas for reactions. Core reflood is assumed to occur such that the clad melt fraction is in the range of 50%.

In analyses of base case scenarios, containment engineered safeguard equipments such as one train of containment sprays and one recirculation fan are assumed available. Failure of a recirculation fan is possible if burning occurs in the upper compartment. Failure of a recirculation fan is treated as a sensitivity case.

In no cases, was there a challenge to the containment integrity. The maximum containment peak pressure of 28 psia appears in CCW sequence as a result of burning in the upper compartment at 6 vol. % H_2 . The containment ultimate pressure capacity is 50.7 psia. The challenge to equipment vital to core recovery are the heat load in the lower compartment. The heat load in the lower compartment is proportional to the lower compartment gas temperature which is which is the resultant of two components, i.e., temperature rise resulting from primary system blowdown and temperature rise resulting from hydrogen combustion. Among all base cases and sensitivity cases, a large LOCA sequence shows the highest peak equipment temperature with a major contribution from the primary system blowdown. This is the case even though the amount of hydrogen burning in the lower compartment is not as much as in other sequences.

Between Unit 1 and Unit 2, the limiting heat load is in Unit 2 due to its larger fuel surface area and higher core power. The failure of the containment air recirculation fan does not provide an additional challenge to containment integrity, and does not indicate a higher heat load on



equipment in lower containment than the Unit 2 large LOCA. Conclusions drawn about the acceptability of the heat loads on vital equipment is beyond the scope of this report.



REFERENCES

- AEPSC, 1981, "Stevenson Report," Attachment 1 to letter AEP:NRC:500A, dated April 7, 1981, R. S. Hunter [I&MECo] to H. R. Denton [NRC].
- AEPSC, 1985, Hydrogen Combustion Modeling Assumptions for D. C. Cook Plant, Attachment to letter AEP:NRC:0500T.
- Baker, L., and Just, L. C., 1962, "Studies of Metal-Water Reactions at High Temperatures III. Experimental and Theoretical Studies of the Zirconium-Water Reaction", ANL-6548.
- Cathcart, J. V., et al., 1977, "Zirconium Metal-Water Oxidation Kinetics IV, Reaction Rate Studies", ORNL/NUREG-17.
- Cronenberg, A. W., 1990, "In-Vessel Zircaloy Oxidation/Hydrogen Generation Behavior During Severe Accidents," NUREG/CR-5597, Engineering Science and Analysis.
- EPRI, 1988, "Large-Scale Hydrogen Combustion Experiments Volume 1: Methodology and Results," EPRI NP-3878.
- Fauske & Associates, 1990, "MAAP 3.0B Users Manual," also, "MAAP 3.0B Complete Code Manual," EPRI NP-777-1 CCML.
- Fauske & Associates, 1991, "D. C. Cook Nuclear Plant Source Term Notebook," FAI/91-178.
- Fauske & Associates, 1992, "Containment Data Collection Notebook, D. C. Cook Nuclear Plant Individual Plant Examination," prepared for American Electric Power Service Corporation.
- Fauske & Associates, 1993, "MAAP 3.0B Code Modification for D. C. Cook 10CFR50.44 Hydrogen Analysis," FAI/93-26.
- Henrie, J. O., 1989, "Timing of the Three Mile Island Unit 2 Core Degradation as Determined by Forensic Engineering," Nuclear Technology, 87, pp. 857-864.
- Hertzbert, M., 1981, "Flammability Limits and Pressure Development in H₂-Air Mixtures," Proc. Workshop on the Impact of Hydrogen on Water Reactor Safety, NUREG/CR-2017, SAND81-0661.
- IDCOR, 1983, "Technical Report 12.1 Hydrogen Generation During Severe Core Damage Sequences."
- Iijima, T., and Takeno, T., 1986, "Effects of Temperature and Pressure on Burning Velocity", Combustion and Flame, Vol. 65, pp. 35-43.
- Liu, D., MacFarlane, R., and Clegg, L., 1981, "Some Results of WNRE Experiments on Hydrogen Combustion", Proc. Workshop on the Impact of Hydrogen on Reactor Safety, NUREG/CR-2017, SAND81-0661.

REFERENCES - Continued

- Luangdilok, W. and Bennett, R. B., "Fog Inerting Effects on Hydrogen Combustion in a PWR Ice Condenser Containment," submitted to 1993 National Heat Transfer Conference, Atlanta.
- Marshall, B. W., 1986, "Hydrogen-Air-Steam Flammability Limits and Combustion Characteristics in the FITS Vessel," Sandia National Laboratories, NUREG/CR-3468, SAND84-0383.
- NUMARC, 1992, "Severe Accident Issue Closure Guidelines", NUMARC91-04.
- Plys, M. G., and Astleford, R. D., 1988, "Modifications for the Development of the MAAP-DOE Code, Volume III: A Mechanistic Model for Combustion in Integrated Accident Analysis Task 3.4.5", DOE/ID-10216, Vol. III.
- SNL, 1985, "Letter from C. Channy Wong (Sandia National Laboratories) to Thomas Crawford (American Electric Service Company)," dated Aug. 12, 1985.
- Tsai, S. S., 1981, "Fog Inerting Analysis for PWR Ice Condenser Plants," Westinghouse Electric Corporation Report.
- Tsai, S. S., and Liparulo, N. J., 1992, "Fog Inerting Criteria for Hydrogen/Air Mixtures," 2nd Int. Workshop on the Impact of Hydrogen on Water Reactor Safety, Albuquerque, New Mexico.
- U.S. NRC, 1990, "Safety Evaluation Report Related to Hydrogen Control Owners Group Assessment of Mark III Containments," U.S. Nuclear Regulatory Commission, NUREG-1417.